


# Comparative clumped isotope temperature relationships in freshwater carbonates

Alexandrea Arnold<sup>1,2</sup>  | John Mering<sup>3</sup> | Lauren Santi<sup>2,3,4</sup> | Cristian Román-Palacios<sup>2</sup> | Huashu Li<sup>5</sup> | Victoria Petryshyn<sup>6</sup> | Bryce Mitsunaga<sup>3</sup> | Ben Elliott<sup>3</sup> | John Wilson<sup>3</sup> | Jamie Lucarelli<sup>2,3,7</sup> | Ronny Boch<sup>8</sup> | Daniel Ibarra<sup>9</sup> | Lin Li<sup>10</sup> | Majie Fan<sup>11</sup> | Darrell Kaufman<sup>12</sup> | Andrew Cohen<sup>10</sup> | Rob Dunbar<sup>13</sup> | James Russell<sup>9</sup> | Stefan Lalonde<sup>14,15</sup> | Priyadarsi D. Roy<sup>16</sup> | Martin Dietzel<sup>8</sup> | Xingqi Liu<sup>5</sup> | Fengming Chang<sup>17</sup> | Robert A. Eagle<sup>1,2,14,18</sup> | Aradhna Tripathi<sup>1,2,3,4,14,18</sup>

## Correspondence

Alexandrea Arnold and Aradhna Tripathi, Department of Atmospheric and Oceanic Sciences, University of California, Los Angeles, Los Angeles, CA, USA.

Email: [ajarnold1@ucla.edu](mailto:ajarnold1@ucla.edu) and [atripathi@ucla.edu](mailto:atripathi@ucla.edu)

## Abstract

Lacustrine, riverine and spring carbonates represent archives of terrestrial climates and their geochemistry has been used to study palaeoenvironments. Clumped isotope thermometry is an emerging tool that has been applied to freshwater carbonates. Limited work has been done to evaluate comparative relationships between clumped isotopes and temperature in different types of modern freshwater carbonates. This study assembles an extensive calibration data set with 135 samples of modern freshwater carbonates from 96 sites and constrains the relationship between independent observations of water temperature and the clumped isotopic composition of carbonates (denoted by  $\Delta_{47}$ ), including new measurements, and recalculates published data in accordance with current community-defined standard values. For temperature reconstruction, the study reports a composite freshwater calibration and material-specific calibrations for biogenic carbonates (freshwater gastropods and bivalves), fine-grained carbonate (e.g. micrites), biologically mediated carbonates (microbialites and tufas) and travertines. Material-specific calibration trends show a convergence of slopes that are in agreement with recently published syntheses, but statistically significant differences in intercepts occur between some materials (e.g. some biogenics, fine-grained carbonates). These differences may arise due to unresolved seasonal biases, kinetic isotope effects and/or varying degrees of biological influence. The impact of different calibrations is shown through application to new data for glacial and deglacial age travertines from Austria and published data sets. While material-specific calibrations may yield more accurate results for biogenic and fine-grained carbonate samples, the use of material-specific and the composite

For affiliations refer to page 21.

This is an open access article under the terms of the [Creative Commons Attribution](https://creativecommons.org/licenses/by/4.0/) License, which permits use, distribution and reproduction in any medium, provided the original work is properly cited.

© 2024 The Author(s). *The Depositional Record* published by John Wiley & Sons Ltd on behalf of International Association of Sedimentologists.

freshwater calibrations generally produces values within 1.0–1.5°C of each other, and typically fall within calibration uncertainty given limitations of precision.

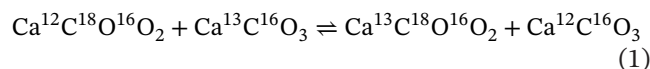
#### KEYWORDS

carbonate clumped isotopes, freshwater calibration, lacustrine carbonates, palaeoclimate reconstruction, riverine carbonates

## 1 | INTRODUCTION

Freshwater sediments can aid in enhancing our understanding of past aquatic systems and their proximal terrestrial environments (Aravena et al., 1992; Schelske & Hodell, 1995; Brenner et al., 1999; Xu et al., 2006; Das et al., 2013; Li et al., 2016; Santi et al., 2020). Of particular interest are carbonate-bearing sediments deposited in freshwater systems, as they are widespread and are sensitive to changes in the local environment, tectonic setting and hydrological conditions, and thus provide a promising archive of continental palaeoclimate information (Arenas-Abad et al., 2010; Gierlowski-Kordesch, 2010; Hren & Sheldon, 2012). However, quantitative temperature proxies for terrestrial carbonate sediments are rela-

Schauble et al., 2006; Hill et al., 2014; Tripathi et al., 2015), with cooler temperatures favouring enhanced combination of  $^{13}\text{C}$  and  $^{18}\text{O}$  within the mineral lattice (i.e. the forward reaction in Equation 1).



This technique measures the abundance of mass-47 isotopologues of  $\text{CO}_2$  gas (containing one or both heavy isotopes [ $^{13}\text{C}$  and/or  $^{18}\text{O}$ ]) liberated from carbonate minerals digested in phosphoric acid. Clumped isotope ratios report the excess of mass-47  $\text{CO}_2$  liberated from a sample relative to predictions for a randomised (stochastic) distribution.  $\Delta_{47}$  is used to describe this excess, as seen in Equation (2), where  $R^i = (\text{mass } i / \text{mass } 44)$ :

$$\Delta_{47} (\text{‰}) = \left[ \left( R^{47} / R^{47}_{\text{stochastic}} - 1 \right) - \left( R^{46} / R^{46}_{\text{stochastic}} - 1 \right) - \left( R^{45} / R^{45}_{\text{stochastic}} - 1 \right) \right] \times 1000 \quad (2)$$

tively scarce. Prior work has explored the use of multiple different proxies to estimate terrestrial temperatures with varying degrees of uncertainty, including soil carbonates, speleothems, fracture veins, ostracods, trace element ratios in lacustrine sediments, tree rings, leaf margin analysis, pollen, biomarkers and noble gases in groundwater (Wilf, 1997; Stute & Schlosser, 2000; Powers et al., 2010; Gallagher & Sheldon, 2013; Esper et al., 2018; Boch et al., 2019; Kaufman et al., 2020; Meckler et al., 2021; Wrožyna et al., 2022), of which only the first five types of proxies are carbonate-associated.

Multiply substituted carbonate ‘clumped’ isotope thermometry represents a promising proxy for reconstructing temperature. The thermodynamic exchange of isotopes among isotopologues of carbonate-containing groups forms the basis for the tracer (Ghosh et al., 2006a, 2006b; Schauble et al., 2006; Hill et al., 2014; Tripathi et al., 2015), with widespread applicability in palaeoclimate, palaeohydrological and palaeoelevation contexts (Csank et al., 2011; Eagle et al., 2013a; Hren et al., 2013; Huntington et al., 2010, 2015; Huntington & Lechler, 2015; Santi et al., 2020; Tripathi et al., 2010, 2014). At equilibrium, the abundance of the multiply substituted isotopologue,  $^{13}\text{C}^{18}\text{O}^{16}\text{O}_2$  relates solely to the formation temperature of the mineral (Ghosh et al., 2006a, 2006b;

An advantage of carbonate clumped isotope-derived temperature estimates is that they are independent of the  $^{18}\text{O}/^{16}\text{O}$  ratio ( $\delta^{18}\text{O}$ ) of the precipitating fluid, as the relevant isotope exchange reaction (Equation 1) takes place within a single phase. Clumped isotope analysis simultaneously measures carbonate  $\delta^{18}\text{O}$  ratios, which allows for the calculation of  $\delta^{18}\text{O}$  values of water at the time of carbonate formation with constraints from  $\Delta_{47}$ -derived temperature estimates (Urey, 1947; Epstein et al., 1953; Vasconcelos et al., 2005).

Past lake and river water temperatures have previously been constrained using clumped isotopes (Huntington et al., 2010, 2015; Kele et al., 2015; Petryshyn et al., 2015; Horton et al., 2016; Hudson et al., 2017; Santi et al., 2020; Li et al., 2021; Wang et al., 2021; Cheng et al., 2022). The additional temperature constraint provided by  $\Delta_{47}$  measurements allows for a calculation of the  $\delta^{18}\text{O}$  values of lake and river waters, which can provide constraints on past hydrology and elevation. The  $\Delta_{47}$ -temperature and  $\Delta_{47}$ -derived water  $\delta^{18}\text{O}$  values in freshwater carbonates and other types of terrestrial archives have in turn been used to evaluate the depiction of various processes in climate models (Eagle et al., 2013a; Tripathi et al., 2014; Santi et al., 2020; Cheng et al., 2022), constrain hydrologic parameters (Santi et al., 2020), and for palaeoaltimetry

(Ghosh et al., 2006a; Huntington et al., 2010, 2015; Ingalls et al., 2017; Li et al., 2019).

However, the accuracy of these reconstructions is fundamentally underpinned by the calibration(s) used for calculations. Thus, this study presents new clumped isotope calibrations derived for freshwater carbonates by synthesising clumped isotope data from 135 samples collected from 96 sites in modern lakes, rivers and springs. New clumped isotope measurements (159 analyses) for 25 new samples from 25 different sites are part of the dataset. This study also includes recalculated published data for samples from 59 sites, on the new reference frame proposed by Bernasconi et al. (2021) that uses carbonate standard values to reduce interlaboratory differences and newer data handling procedures (Daëron, 2021). Measurements from 12 sites presented on the new reference frame in another publication are also included (Anderson et al., 2021).

Recently published syntheses have limited freshwater carbonate data; the synthesis from Petersen et al. (2019) had no freshwater carbonates, and Anderson et al. (2021) had 16 carbonates (tufas and travertines) of which seven samples were from  $T < 10^{\circ}\text{C}$ , and six samples were from  $T > 30^{\circ}\text{C}$ . Most clumped isotope studies of freshwater carbonates have analysed a small number of samples (Huntington et al., 2010, 2015; Kele et al., 2015; Petryshyn et al., 2015; Grauel et al., 2016; Horton et al., 2016; Zaarur et al., 2016; Hudson et al., 2017; Kato et al., 2019; Santi et al., 2020; Anderson et al., 2021; Li et al., 2021; Wang et al., 2021); some do not report calibrations, are not in the updated reference frame, and/or utilise different methods for constraining modern water temperatures. Of these 12 studies reporting data for modern freshwater carbonates, five report new data for <five samples, while nine have data for <11 samples. Only four studies have larger numbers of samples ( $n = 25\text{--}33$ ). The smaller size of most published data sets means that there are few calibration constraints on certain types of lacustrine carbonates, such as freshwater gastropods, and that the similarities or differences between different types of lacustrine carbonates is poorly known. In marine carbonates, which have been more extensively studied, there is a body of literature supporting material specificity or kinetic effects in some archives (e.g. coral, echinoderms; cf. Ghosh et al., 2006a, 2006b; Saenger et al., 2012; Kimball et al., 2016; Spooner et al., 2016; Davies & John, 2019). Additionally, possible influences of seasonal and temperature biases in carbonate formation are likely to be important for lacustrine carbonates (Hren & Sheldon, 2012; Horton et al., 2016), as might kinetic effects given the range of freshwater ionic compositions (Hill et al., 2014, 2020; Tripathi et al., 2015).

The freshwater carbonate data set synthesised for this study contains new, recalculated and recently published data used to examine clumped isotope signatures in travertines,

fine-grained carbonates, biogenic (freshwater molluscs) and biologically mediated (tufas and microbialites) carbonates to provide a foundation for intercomparison and calibration of carbonate clumped isotope results from terrestrial aquatic systems. Sample localities within this study are geographically diverse, and include equatorial, mid-latitude and polar sites at a variety of elevations and climates. This study presents a composite freshwater calibration and material-specific calibrations for different carbonate types for community use. The impact of the calibrations derived in this study on reconstructed water temperature and source water  $\delta^{18}\text{O}$  values in both modern and past contexts is also assessed.

## 2 | MATERIALS AND METHODS

### 2.1 | Sample and site selection

The data set presented in this study includes carbonate materials selected to represent modern lacustrine surface water conditions. For lakes, biogenic and biologically mediated samples selected for analysis are types that grow nearshore or occupy the photic zone above the thermocline. Additionally, this analysis includes fine-grained carbonates due to their formation occurring in surface waters, where evaporation and photosynthesis have the strongest effect on water chemistry (Platt & Wright, 2009; Gierlowski-Kordesch, 2010; Hren & Sheldon, 2012).

This synthesis includes locations where modern surface water temperatures are available in publications (Table S2). Temperatures reflect the typical season of carbonate formation for each carbonate type. For sites where multiple years of hydrographic data are available, temperature variability indicates one standard deviation of the monthly average temperatures during the typical season of carbonate formation for each type of carbonate (see Text S1; Table S2). If less than a year of data is available for a site, then given there is year-to-year variability in temperatures, two standard deviations of available measurements are reported. To estimate errors for lake temperatures for data from Li et al. (2021), this study propagates the standard error of the regression and the temperature error from the original publication in quadrature. Sites with only a season average value available or a measured temperature value without reported uncertainty do not have data constraining seasonal variations in temperature and use an assumed uncertainty of  $\pm 2^{\circ}\text{C}$ , the average standard deviation observed for localities in this study with well-constrained temperatures. This approach to error estimation is conservative in some settings and not in others, as seasonal temperature variation varies based on the location and properties of each lake system. For example, low-elevation

lakes in the tropics experience less monthly temperature variation while high-elevation, high-latitude lakes experience larger fluctuations in temperature. Most lakes in this synthesis reside within the low to mid-latitudes, with most site elevations under 2 km; thus, the assignment of error represents an average for this data set (Figure S1). Since temperature uncertainty for these samples is variable and is calculated in different ways, the models used to derive relationships for this study do not use them, but the temperature uncertainties are shown in figures to visualise ranges of uncertainty.

## 2.2 | Sample preparation

### 2.2.1 | Biogenic carbonates

Aquatic gastropod and bivalve shells were first separated by taxon and cleaned of organic material by scraping and sonicating in Milli-Q deionised water. Samples were dried overnight at 50°C, and complete shells were powdered using a mortar and pestle, and reacted with 3% hydrogen peroxide for 60 min to remove any remaining organic material (Eagle et al., 2013b). Depending on carbonate content of the gastropod and bivalve shells and instrument sensitivity at the time of analysis, the amount of sample used for mass spectrometric analysis varied between 5 and 10 mg for a single replicate.

### 2.2.2 | Fine-grained carbonates

Samples of unconsolidated calcareous particles were disaggregated in Milli-Q deionised water, after which the mixture was poured through a 212 µm steel mesh filter and left to settle in a beaker for 10 min. The residue was poured into a second beaker after filtration to remove any remaining suspended material, and this process was repeated until virtually no observable settling occurred. The final residue was treated with 3% hydrogen peroxide for 60 min to remove any remaining organic material (Eagle et al., 2013b). Resulting fine-grained carbonate was collected on a filter and dried at 50°C. Depending on carbonate content and instrument sensitivity, the amount of sample used for mass spectrometry varied between 10 and 30 mg for a single replicate.

### 2.2.3 | Biologically mediated carbonates

Tufas and microbialites were cut perpendicular to laminae, and polished slabs and thin sections were prepared to target specific zones for analysis. Samples were ground into a fine powder using a microdrill. To

prevent potential solid-state isotopic reordering of C-O bonds due to frictional heating, the drilling during this process was limited in duration and speed (rpm). Between 5 and 15 mg of sample were treated with 3% hydrogen peroxide for 60 min to ensure the removal of any organics and dried overnight at 50°C (Eagle et al., 2013b).

## 2.3 | Stable isotope measurements

All samples were analysed at the University of California, Los Angeles on a Thermo 253 Gas Source isotope ratio mass spectrometer in the Eagle-Tripati Laboratory between 2012 and 2019, primarily between 2013 and 2015. Sample introduction and measurement procedures are described in detail in Upadhyay et al. (2021), with sample size varying depending upon the carbonate content. Briefly, carbonate samples were first reacted with 105% phosphoric acid for 20 min on a 90°C on-line common acid bath system, whereby solid carbonate reacted to produce CO<sub>2</sub> gas for analysis. Acid temperature was monitored with a thermocouple throughout each analysis and checked daily for drift. Each sample gas was cryogenically purified using an automated purification system that was modelled on the previously described system at the California Institute of Technology (Passey et al., 2010) in the Eiler laboratory. The liberated gas from each sample passed through two separate gas traps to ensure the removal of water and other compounds: the first (containing ethanol) is kept at -76°C by dry ice, and the second (containing liquid nitrogen) is kept at -196°C. Next, the sample gas is passed through silver wool to remove sulphur compounds (e.g. halocarbons and hydrocarbons; Spencer & Kim, 2015) and remaining trace contaminants were separated by moving the resultant gas through a Thermo Trace GC Ultra gas chromatograph column, which is filled with a divinyl benzene polymer trap, Porapak Q at -20°C (Tripati et al., 2015; Santi et al., 2020). The purified sample gas was passed on to the mass spectrometer for analysis.

Data were collected over nine blocks, each consisting of 10 comparisons of the sample and reference gases, with the mean ratios from each block used to determine δ<sup>13</sup>C, δ<sup>18</sup>O, Δ<sub>47</sub>, Δ<sub>48</sub> and Δ<sub>49</sub> values of the gas. During each acquisition on the mass spectrometer, sample isotope values were measured relative to high purity Oztech brand CO<sub>2</sub> reference gas (δ<sup>18</sup>O = 25.03‰ VSMOW, δ<sup>13</sup>C = -3.60‰ VPDB). Each run was started with an equilibrated CO<sub>2</sub> gas standard of varying composition and temperature (25 and 1000°C), which were used along with ETH-1 and ETH-2 to correct for non-linearity. Carbonate standards, including the ETH suite from Bernasconi et al. (2021) and in-house standards described in Upadhyay et al. (2021) and Lucarelli et al. (2023), were run every two to four analyses

and used for the empirical transfer function for projection into the I-CDES reference frame. Accepted standard values used for corrections are from Bernasconi et al. (2021) for all ETH standards and from Lucarelli et al. (2023) for all in-house carbonate standards. Averages for standard values in this study can be found in Table S3. At least three replicate analyses of each sample were performed, unless insufficient material limits the number of analyses.

## 2.4 | Data handling

The replicate level values for new and reprocessed samples are archived in the EarthChem database.

### 2.4.1 | New data

Table S1 reports isotopic data for samples used within this study. Detailed information about data processing can be found in Upadhyay et al. (2021). Data are reported on the I-CDES scale which projects values into a 90°C reference frame, following recommendations from Bernasconi et al. (2021). Acid digestion fractionation factors used for calcite and aragonite  $\delta^{18}\text{O}$  values are from Swart et al. (1991) and Kim et al. (2007), respectively; for calculation of water  $\delta^{18}\text{O}$  values, the equation from Kim and O'Neil (1997) was used for calcite and the equation from Kim et al. (2007) was used for aragonite. For samples measured in the Eagle-Tripati laboratory, data were processed using *Easotope* (Daëron et al., 2016; John & Bowen, 2016) and is included in the supplement, and archived on EarthChem. Replicated measurements were excluded if results were consistent with high organic content, as indicated by anomalous  $\Delta_{48}$  or  $\Delta_{49}$  values for a given correction interval, with samples having values that are more than  $3\sigma$  from the replicate mean being flagged for possible exclusion (Upadhyay et al., 2021). Replicates were also excluded if they had anomalous values of  $\Delta_{47}$  (I-CDES),  $\delta^{13}\text{C}$  (VPDB) and  $\delta^{18}\text{O}$  (VPDB) values, of more than  $3\sigma$  from the remaining replicates, which can reflect incomplete digestion or contamination (Tripati et al., 2015). If less than three replicates were run for a sample, uncertainty of the reported value was determined by propagating both the internal reproducibility of the sample and the average external reproducibility of the samples in this study.

### 2.4.2 | Data from prior studies

Detailed information about each data set can be found in the original publication and the methodology for including these values in this study is as follows:

Anderson et al. (2021): Data are presented in the I-CDES reference frame.

Bernasconi et al. (2018): In their study, the  $\Delta_{47}$  values from Kele et al. (2015) was reprocessed using the Brand parameter set. Their results were presented in CDES, but projected into I-CDES using the following equation from Bernasconi et al. (2021):

$$\Delta_{47} (\text{I-CDES, } \text{‰}) = -0.035545 - 0.000180 \delta_{47} + 0.942483 \Delta_{47} (\text{CDES}_{25}) \quad (3)$$

Huntington et al. (2010, 2015); Petryshyn et al. (2015): The  $\Delta_{47}$  measurements for these studies were completed in the Eiler laboratory at CalTech. Samples from these studies were either digested independently at 25°C and collected in break seals or in a common acid bath at 90°C for analysis in the mass spectrometer. For samples at 90°C, an acid fractionation factor of 0.088‰ was used to project into the CDES reference frame at 25°C (Petersen et al., 2019). Sample and standard data from Caltech for these studies were imported into *Easotope* for data processing on the CDES reference frame (John & Bowen, 2016). Data were reprocessed using the Brand parameter set. Non-linearity in the mass spectrometer was corrected using 1000°C equilibrated gases with varying bulk compositions. The empirical transfer function was constructed using both carbonates and gas standards. Table S3 reports mean standard values associated with these analyses. Accepted standard values used for corrections came from processing I-CDES values in Lucarelli et al. (2023) into the CDES reference frame. The following equation projects these measurements into the I-CDES reference frame based on the methodology in Bernasconi et al. (2021):

$$\Delta_{47} (\text{I-CDES, } \text{‰}) = -0.034927 - 0.000181 \delta_{47} + 0.942466 \Delta_{47} (\text{CDES}_{25}) \quad (4)$$

Li et al. (2021); Wang et al. (2021): Clumped isotope data from this study were generated in the Eagle-Tripati laboratory. Data were reprocessed in *Easotope* (John & Bowen, 2016) using updated values for the ETH standards from Bernasconi et al. (2021). Samples from Wang et al. (2021) were updated to the Brand parameter set. Data were processed identically to the original studies.

## 2.5 | Regression methodology

Recent work has shown that models derived using ordinary least squares (OLS) perform better, under synthetic data sets comparable to the one assembled in this study (<500 samples), than their error-in-variables counterparts (e.g. York regression, Deming regression). The OLS has higher accuracy and precision for regression parameters, and

performs similar to Bayesian simple linear models for both calibration of clumped isotopes and for temperature reconstruction (Román Palacios et al., 2021). This study evaluates the relationship between  $\Delta_{47}$  and growth temperature using OLS regression models fit in the `lm` R function in the stats package (R Core Team, 2022). Due to the varying temporal resolution of the independently measured water temperatures and lack of long-term temperature records for some sites, this study uses an OLS regression model instead of an errors-in-variables model. Table S1 shows the calibration data used to derive regressions for the entire data set (a composite freshwater calibration), and material-specific calibrations for biogenic carbonates (bivalves and gastropods), biologically mediated carbonates (microbialites and tufas), fine-grained carbonates and travertines.

An analysis of covariance (ANCOVA) allows for evaluation of material specificity within this data set and comparison of the derived regression parameters to other studies by analysing pairwise differences in slopes and intercepts between groups of data. This study compares four different calibrations: the composite calibration, which includes all data from this study, along with the material-specific calibrations, a recently published calibration

that includes natural and synthetic samples (Anderson et al., 2021) and a ‘universal’ calibration created from a synthesis of clumped isotope calibration studies (Petersen et al., 2019). Comparisons to previously published calibration equations are also shown, with data brought into the 90°C reference frame here using acid fractionation factor values reported in Petersen et al. (2019), which yield similar values given that both reference frames are considering acid fractionation at 90°C.

### 3 | RESULTS

#### 3.1 | $\Delta_{47}$ -Temperature Relationships

Samples in this study are from modern lakes (including playas), rivers and springs, from geographically and climatically diverse settings (Figure 1; Table S1). Table S1 contains the calibration data used to derive regressions for the entire dataset (a composite freshwater calibration), and material-specific calibrations for biogenic carbonates (bivalves and gastropods), biologically mediated carbonates (microbialites and tufas), fine-grained

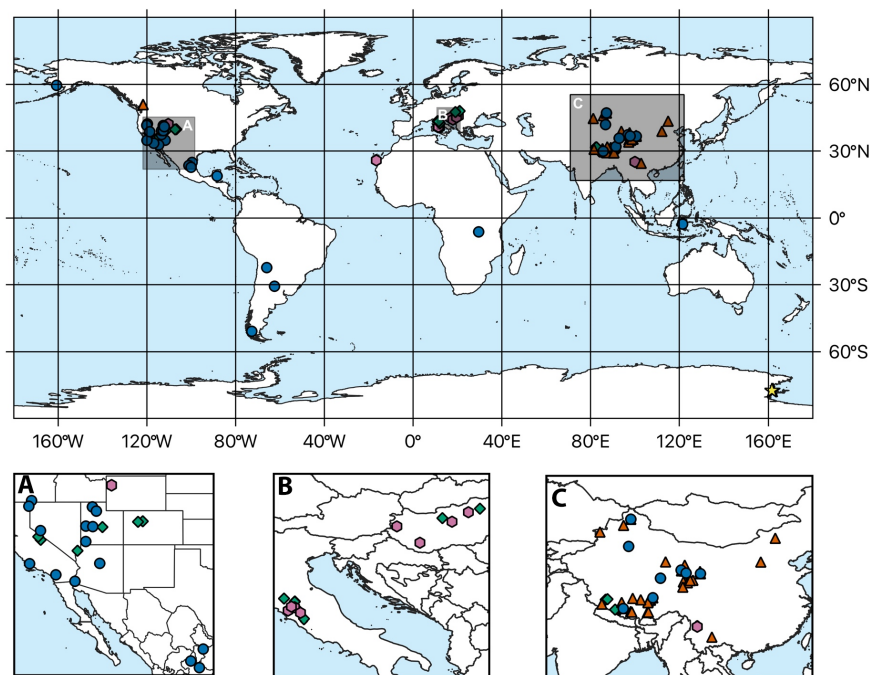


**FIGURE 1** Sample locations used for this study. Clumped isotope data in this study come from 135 samples collected from 96 sites in modern lakes, rivers and springs. Blue circles indicate the location of samples with new data from the Eagle-Tripati laboratory ( $n=25$ ; 159 measurements), orange triangles indicate data measured in the Eagle-Tripati laboratory that has been published and recalculated onto the I-CDES reference frame for this study ( $n=30$ ), green diamonds indicate data from other laboratories recalculated onto the I-CDES reference frame as part of this study ( $n=29$ ), pink hexagons denote sites where samples are analysed twice, with one set of measurements being recalculated and the other taken directly from published data ( $n=12$ ), yellow stars represent data directly taken from other publications ( $n=3$ , points overlap on the main figure).

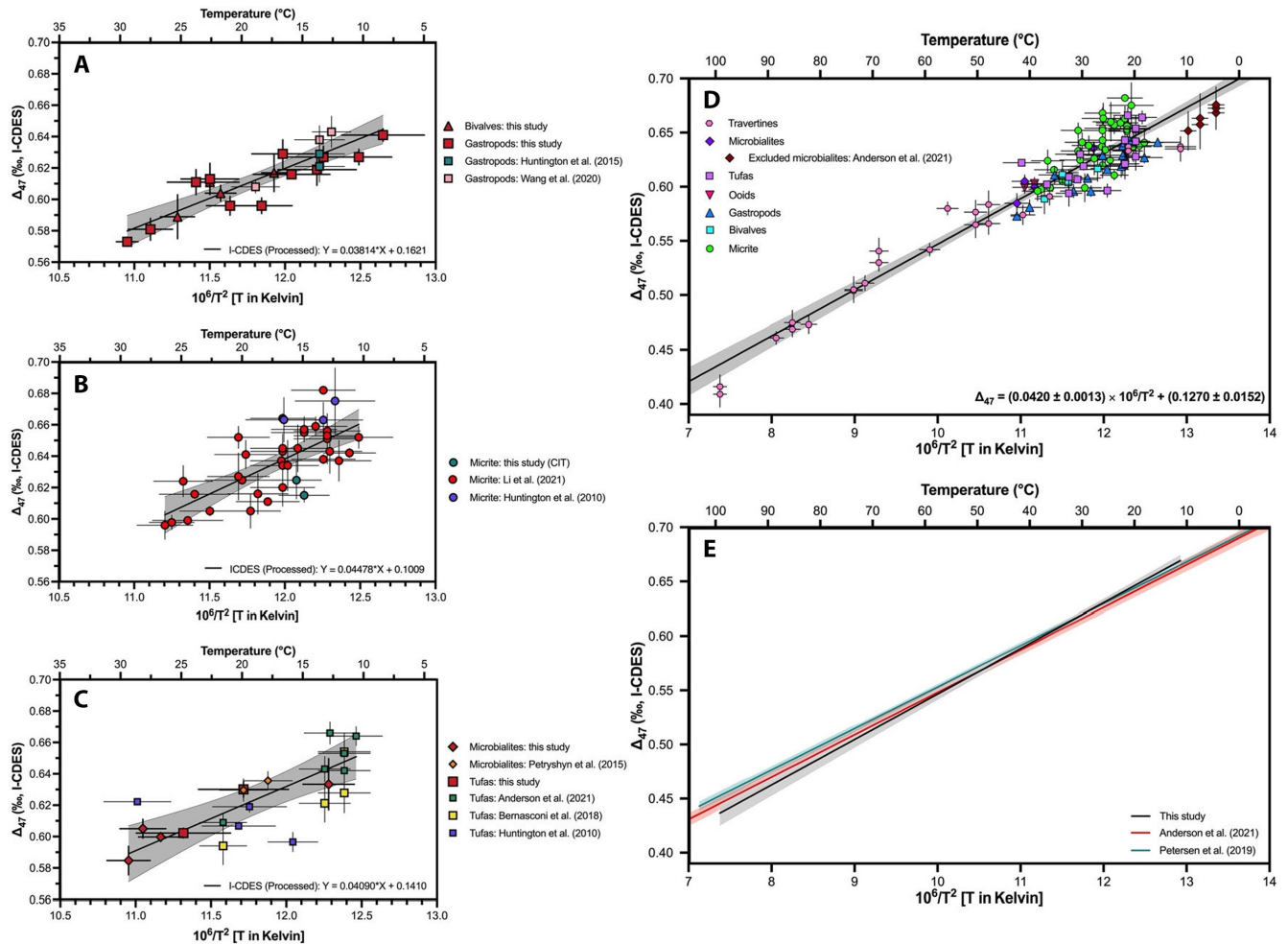


**FIGURE 2** (A–C) Calibration data by study for (A) biologic carbonates, (B) fine-grained carbonates and (C) biologically mediated carbonates. Regressions are shown for data reprocessed in the I-CDES reference frame. Symbols shaded in red colours indicate samples processed in the Eagle-Tripati laboratory. (D)  $\Delta_{47}$ -temperature relationship for all 108 freshwater carbonates included in this study. Black line represents a linear, ordinary least squares regression through the data and the grey-shaded area represents the 95% confidence interval. A strong relationship is present between  $\Delta_{47}$  and temperature ( $p < 0.0001$ ;  $r^2 = 0.8959$ ). Red diamonds represent low temperature and/or high pH lacustrine microbialites from Anderson et al. (2021) excluded from the regression. (E) Comparison of the composite freshwater regression determined here to previously published clumped isotope calibrations. ANCOVA results show that the slope derived for the calibration is statistically different from the acid-corrected calibration of Petersen et al. (2019) and Anderson et al. (2021), with  $p_{\text{slope}}$  values of 0.0036 and 0.0334, respectively (Table 2).

**TABLE 1** Derived regression parameters for all freshwater calibration data and material-specific calibration data using linear, ordinary least squares regression.

	<i>n</i>	Slope ± 1 s.e.	Intercept ± 1 s.e.	<i>r</i> <sup>2</sup>	<i>p</i>
Composite	108	0.0420 ± 0.0013	0.1270 ± 0.0152	0.9053	<0.0001
Biogenic	23	0.0371 ± 0.0043	0.1739 ± 0.0510	0.7811	<0.0001
Fine-grained	38	0.0462 ± 0.0074	0.0844 ± 0.0890	0.5170	<0.0001
Bio-mediated	22	0.0345 ± 0.0067	0.2164 ± 0.0798	0.5669	<0.0001
Travertine	23	0.0398 ± 0.0020	0.1450 ± 0.0203	0.9487	<0.0001

carbonates and travertines. The  $\Delta_{47}$  values for samples within this study range from 0.409 to 0.682‰ with independently measured water temperatures ranging from 5 to 95°C. Figure 2 and Table 1 present calibrations derived in this study.

### 3.2 | Comparative regression models for different materials

This study constructs calibrations for biogenic carbonates (bivalves and gastropods), biologically mediated

TABLE 2 Results of the ANCOVA test for calibration-pairs for slope and intercept.

<b>Regression parameter: slope</b>							
	This study: composite <sup>a</sup>	This study: biogenic	This study: fine-grained	This study: bio-mediated <sup>a</sup>	This study: travertine	Petersen et al. (2019) <sup>b</sup>	Anderson et al. (2021) <sup>a</sup>
This study: composite <sup>a</sup>						0.0036	0.0334
This study: biogenic			0.4880	0.7463	0.6730	0.9456	0.7660
This study: fine-grained <sup>a</sup>		0.4880		0.3785	0.6114	0.4590	0.4880
This study: bio-mediated <sup>a</sup>		0.7463	0.3785		0.4580	0.6770	0.4852
This study: travertine		0.6730	0.6114	0.4580		0.3620	0.6320
Petersen et al. (2019) <sup>b</sup>	0.0036	0.9456	0.4590	0.6770	0.3620		0.2078
Anderson et al. (2021) <sup>a</sup>	0.0334	0.7660	0.4880	0.4852	0.6320	0.2078	
<b>Regression parameter: intercept</b>							
	This study: composite <sup>a</sup>	This study: biogenic	This study: fine-grained	This study: bio-mediated <sup>a</sup>	This study: travertine	Petersen et al. (2019) <sup>b</sup>	Anderson et al. (2021) <sup>a</sup>
This study: composite <sup>a</sup>							
This study: biogenic			0.0000	0.0047	0.6320	0.0728	0.2710
This study: fine-grained		0.0000		0.0379	0.0050	0.0000	0.0000
This study: bio-mediated <sup>a</sup>		0.0047	0.0379		0.1140	0.2540	0.0542
This study: travertine		0.6320	0.0050	0.1140		0.0354	0.4440
Petersen et al. (2019) <sup>b</sup>	0.0036	0.9456	0.4590	0.6770	0.3620	0.2078	0.0835
Anderson et al. (2021) <sup>a</sup>	0.0334	0.7660	0.4880	0.4852	0.6320	0.2078	

Note: Red shading indicates differences in parameters with 95% confidence ( $p < 0.05$ ), yellow shading indicates differences in parameters with 90% confidence ( $0.05 < p < 0.10$ ) and no shading indicates no statistically significant difference between parameters. Top: ANCOVA results for slope. 27 pairs have a  $p > 0.1$ , demonstrating a convergence of slope when looking at material-specific groups of data. Bottom: Results of the ANCOVA test for calibration-pairs for intercept. This analysis is only performed on calibration pairs that had  $p$ -values exceeding 0.1 for the slope analysis. Differences in intercepts between different groups of data in this study were prevalent in four pairwise comparisons ( $p < 0.05$ ); thus, material-specific calibrations may be appropriate for climate reconstructions.

<sup>a</sup>Composite and biologically mediated regression excludes low temperature/high pH microbialites from Anderson et al. (2021).

<sup>b</sup> $\Delta_{47}$  values are shown in a 90°C reference frame using AFF presented in Petersen et al. (2019).



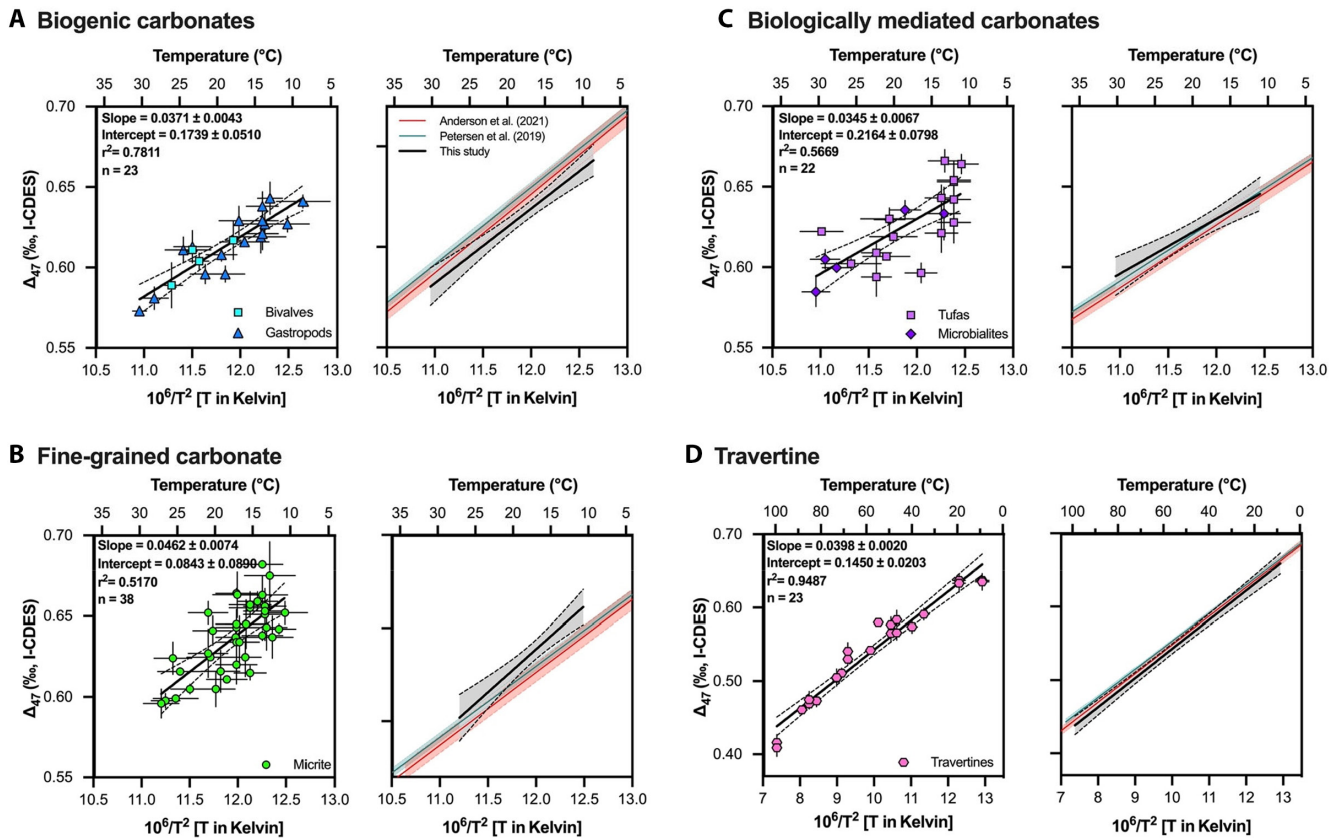


**FIGURE 3**  $\Delta_{47}$ -temperature relationships for (A) biogenic carbonates, (B) fine-grained carbonates, (C) biologically mediated carbonates and (D) travertines. Left:  $\Delta_{47}$ -temperature relationship for all carbonate types included in this study. Black line represents a linear, ordinary least squares regression through the data. A strong relationship between  $\Delta_{47}$  and temperature exists for each group of data. All groups of data have statistically indistinguishable slopes, but find statistically significant differences in intercepts between a majority of data sets (Table 2), suggesting that material-specific calibrations may be most appropriate. Right: Derived comparison of the material-specific calibrations to previously published clumped isotope calibrations. All material-specific regressions derived in this study have statistically similar slopes to the slopes presented in Petersen et al. (2019) and Anderson et al. (2021), but significant differences in intercept (Table 2).

carbonates (microbialites and tufas), fine-grained carbonates and travertines. This study tests if there is material specificity in  $\Delta_{47}$ -temperature relationships and evaluates whether regression parameters are significantly different between these groups of materials (Tables 1 and 2; Figure 3).

### 3.2.1 | Biogenic carbonates

The biogenic carbonate calibration uses 137 analyses from 23 samples, with  $\Delta_{47}$  values ranging from 0.573 to 0.643‰ and independently constrained water temperatures ranging from 7 to 29°C. This data set includes 16 new samples, alongside reprocessed data from Huntington et al. (2015) and Wang et al. (2021) updated onto the I-CDES reference frame. This calibration shows a significant temperature dependence (Figure 3A;  $r^2 = 0.7811$ ,  $p < 0.0001$ ).

### 3.2.2 | Fine-grained carbonates

This study presents two new samples of fine-grained carbonates, in addition to reprocessed data from three samples from Huntington et al. (2010) and 33 samples from Li et al. (2021) onto the I-CDES reference frame. Fine-grained carbonates in this study include water temperatures between 9.8 and 29.0°C and  $\Delta_{47}$  values from 0.596 to 0.682‰. Fine-grained carbonates evaluated in this study demonstrate a significant degree of variability (Figure 3B;  $r^2 = 0.5170$ ).

### 3.2.3 | Biologically mediated carbonates

The calibration for biologically mediated carbonates uses results from 255 analyses of 24 samples, including seven new samples, 13 reprocessed samples from Bernasconi et al. (2018), Huntington et al. (2015, 2010), Petryshyn

et al. (2015) and Santi et al. (2020) converted into I-CDES, and four samples from Anderson et al. (2021). Water temperatures for biologically mediated samples span 18.9°C (10.1–29.0°C) and  $\Delta_{47}$  values range between 0.585 and 0.666‰. The data set exhibits significant variability (Figure 3C;  $r^2 = 0.5669$ ) and a significant relationship between  $\Delta_{47}$  and temperature is present ( $p < 0.0001$ ).

### 3.2.4 | Travertines

The regression for travertine samples uses results from 543 analyses of 23 samples. The travertine data set includes 15 recalculated samples from previous publications projected onto the I-CDES reference frame (Kele et al., 2015; Bernasconi et al., 2018) following methodology in the supplement of Bernasconi et al. (2021) and eight new published measurements (Anderson et al., 2021). Travertine samples encompass the largest range of independently measured water temperatures (5–95°C) and  $\Delta_{47}$  values (0.409–0.637‰). Similar to the other groups of carbonates considered in this study, the data show a significant temperature dependence (slope;  $p < 0.0001$ ) and a high degree of agreement between the fitted values and calibration data points ( $r^2 = 0.9487$ ). When restricting travertines to cover the same temperature range as other carbonate groups analysed in this study, the  $r^2$  value is highest relative to other groups investigated in this study ( $r^2 = 0.88$ ). However, this analysis only contains six samples within the restricted temperature range and result in a shallower slope (0.0330) and higher intercept (0.2171) relative to the calibration derived from all travertines.

## 4 | DISCUSSION

### 4.1 | Comparison of material-specific and composite freshwater calibrations

#### 4.1.1 | Composite freshwater calibration

The freshwater composite calibration slope derived within this study yields a statistically significant difference in slope to that of the ‘universal’ calibration derived in Petersen et al. (2019) (projected into a 90°C reference frame) (Figure 2E;  $p_{\text{slope}} = 0.0036$ ; Table 2). Similarly, the freshwater composite calibration derived in this study results in a steeper slope and shallower intercept than the recently published Anderson et al. (2021) calibration. Although the 95% confidence intervals on the estimated regression models overlap visually (Figure 2E), an

ANCOVA shows that the slopes for the two calibrations are significantly different from each other ( $p_{\text{slope}} = 0.0334$ ; Table 2), with the slope for the composite regression in this study being steeper relative to those derived in the prior publications (Figure 2E).

Anderson et al.'s (2021) calibration includes low-temperature Antarctic microbialites that are offset from other data, with half of the samples from a high pH (10.3–10.7; Mackey et al., 2018) environment (Figure 2D). Low temperature and high pH are environmental factors that could give rise to potential kinetic isotope effects or DIC speciation effects (Tang et al., 2014; Tripathi et al., 2015). In fact, all of the Antarctic samples are negatively offset from the rest of the data in this study, and thus, these data are excluded from both the composite and the biologically mediated regressions reported here (Table 1). These patterns (the offset of the Anderson et al., 2021 data from other data) hold up when comparing results to only the recent measurements, and the broader freshwater composite calibration (Table S4).

Table S5 shows the range of temperatures derived using different calibrations for  $\Delta_{47}$  values ranging from 0.550 to 0.700‰, in 0.025‰ increments.

#### 4.1.2 | Biogenic carbonates

Biogenic carbonates record lower  $\Delta_{47}$  values relative to the regression derived from all freshwater carbonates in this study (Figure 2D). The depletion in  $\Delta_{47}$  values observed within these samples relative to fine-grained carbonates, travertines and biologically mediated carbonates could stem from changes in growth rate as a function of season, or other unidentified factors. As the sample size requirements for clumped isotopes are relatively large, it often requires the analyses of either a complete shell or the majority of a shell, effectively integrating seasonal signals recorded in the shell and potentially leading to a more muted temperature sensitivity of the calibration in comparison to seasonally resolved sampling. There may also be a mismatch of independently measured in situ measured water temperatures, which is representative of a multi-year average, and the temperature range experienced by biologic samples, which typically have a shorter lifespan and thus, a shorter timeline for shell growth. Another possibility is that kinetic isotope fractionations may manifest in freshwater gastropod and bivalve shells, as have been shown in prior work on marine biogenic carbonates such as coral skeletons (Ghosh et al., 2006a, 2006b; Saenger et al., 2012).

An ANCOVA analysis finds significant differences in intercepts between biogenic carbonates and fine-grained

carbonates ( $p_{\text{intercept}} < 0.0001$ ) and biologically mediated carbonates ( $p_{\text{intercept}} = 0.0047$ ; Table 2), but no statistical difference in slopes between the  $\Delta_{47}$ -T regression of biogenic carbonates and other carbonate groups within this study (Table 2). This pattern is consistent when examining the data set as a whole, or only the UCLA measurements of biogenic carbonates relative to both UCLA measurements of fine-grained carbonates and biologically mediated carbonates (Table S4). However, differences between slopes derived for other carbonate groups in this study and biogenic carbonates are as large as 0.0091, which has implications for temperature reconstructions (Table S5). Regression parameters for biogenic carbonates derived in this study are of intermediate slope and intercept relative to other materials (Table 1).

When comparing the biogenic calibration to the calibrations presented in Anderson et al. (2021) and Petersen et al. (2019), an ANCOVA indicates no difference in slope between these studies and the biogenic carbonate calibration, but shows differences in intercept between this study and the calibration derived by Petersen et al. (2019) ( $p_{\text{intercept}} = 0.0728$ ) (Figure 3A; Table 2). Biogenic carbonates in this study show offsets to lower  $\Delta_{47}$  values relative to the published calibrations discussed here (Figure 3A). Reconstructions using the biogenic regression determined here result in consistently lower temperatures than those derived with the calibrations of Anderson et al. (2021) and Petersen et al. (2019) throughout the range of  $\Delta_{47}$  values in this data set.

Measured  $\Delta_{47}$  and  $\delta^{18}\text{O}_{\text{carbonate}}$  values do not show a significant relationship (Figure S2). Furthermore, there is no significant relationship between  $\Delta_{47}$  and  $\delta^{18}\text{O}_{\text{carbonate}}$  residual values (relative to equilibrium estimates) (Figure S3). Future research could examine whether kinetic effects affect the  $\Delta_{47}$  values of freshwater biogenic carbonates. Specifically, dual  $\Delta_{47}$ - $\Delta_{48}$  measurements (Lucarelli et al., 2023) could help identify if there were kinetic effects expressed in these and other types of freshwater carbonates. Data for culture experiments at controlled temperatures as well as comparison with other geochemical indicators could also identify kinetic effects.

#### 4.1.3 | Fine-grained carbonates

The  $\Delta_{47}$ -temperature relationship for fine-grained carbonates analysed in this study has multiple sources of uncertainty. One factor that contributes to variability in  $\Delta_{47}$  values in fine-grained freshwater carbonates is potentially due to uncertainty in the timing of surface carbonate precipitation events at each site. Biological processes, such as algal blooms and temperature effects, which can peak at different times throughout the year, can

enhance authigenic carbonate precipitation. However, timing of carbonate precipitation events varies depending on the characteristics of each lake system (i.e. open or closed, location, stratification/ventilation, etc.; Hren & Sheldon, 2012).

A second factor is that fine-grained carbonate lake sediments may have a mixture of sources, including authigenic carbonate precipitation, fragments of biogenic carbonates and detrital carbonates deposited at the sampling location. In particular, ostracod valves in some samples may be a source of scatter seen since the timing of formation for fine-grained carbonates and ostracods may be different. Since different factors control organism growth, the inclusion of potential fragments of fossilised material may bias temperature estimates derived by clumped isotope analysis. The majority of the samples in this synthesis are from Li et al. (2021), who filtered samples through a 45  $\mu\text{m}$  mesh and also screened for ostracod valves. New samples measured for this study were obtained by sieving through 212  $\mu\text{m}$  mesh, and thus, there may be fragments of juvenile or mature ostracods. The publication from Huntington et al. (2010) does not report if there was any screening for bioclastic fragments.

Detrital influences may be another source of the variability observed in the  $\Delta_{47}$ -temperature relationship for fine-grained carbonates. Catchment-derived carbonate is likely to be recording different conditions than authigenic carbonate precipitated in the water column and could bias  $\Delta_{47}$  results depending on the formation temperature and the relative proportion of authigenic and detrital carbonate inputs. To minimise the delivery of catchment material to the sampling site, locations for sampling in Li et al. (2021) were at least 2 km from the lake shoreline or from the middle of each lake (when possible). Inclusion of detrital material, in particular at lower carbonate content, would play more of a role in biasing  $\Delta_{47}$  content. However, there is no significant relationship with dilution from terrigenous material as indicated by carbonate content (Figure S4). However, data from other sources did not evaluate detrital contributions. Future work with authigenic carbonates would benefit from other methods, such as scanning electron microscopy, to evaluate detrital input.

The calibration derived from fine-grained carbonates results in the steepest slope and shallowest intercept derived in this study (Table 1). When comparing the derived fine-grained carbonate parameters to other carbonate groups in this study, an ANCOVA shows no significant difference in slopes is found between carbonate materials, but significant differences in intercept is observed between fine-grained carbonates and biogenic carbonates ( $p_{\text{intercept}} < 0.0001$ ), biologically mediated carbonates ( $p_{\text{intercept}} = 0.0379$ ), and travertines ( $p_{\text{intercept}} = 0.0050$ ). No statistical difference between

regressions is found when using the entire fine-grained carbonate data set relative to a regression constructed only using fine-grained carbonates measured at UCLA. Additionally, the results of the ANCOVA indicate differences in regression parameters between the same groups when looking at the entire fine-grained carbonate data set and the fine-grained carbonate data set measured at UCLA (Table 2; Table S4).

Visually, the fine-grained carbonates regression is positively offset relative to both the Anderson et al. (2021) and Petersen et al. (2019) calibrations (Figure 3B); however, an ANCOVA shows agreement in slope between all three regressions reveals significant differences in intercept between the calibration from Petersen et al. (2019) ( $p_{\text{intercept}} < 0.0001$ ) and a recently published calibration on the I-CDES scale (Anderson et al., 2021;  $p_{\text{intercept}} < 0.0001$ ). Applying these calibrations to the range of  $\Delta_{47}$  values in the fine-grained data set produces consistently lower values relative to the fine-grained carbonate regression derived in this study.

Fine-grained carbonates in this study show an average positive offset of 0.012‰ in residual  $\Delta_{47}$  values relative to estimated equilibrium values from Lucarelli et al. (2023) (Figure S3). There is no statistically significant relationship between residual  $\Delta_{47}$  and residual  $\delta^{18}\text{O}_{\text{carbonate}}$  values, consistent with equilibrium, and with prior work reporting that authigenic carbonates precipitate near equilibrium and carbonate precipitation rate or water chemistry do not impact their  $\Delta_{47}$  values (Li et al., 2020).

#### 4.1.4 | Biologically mediated carbonates

Application of the biologically mediated regression results in warmer estimated temperatures, particularly at higher temperatures, relative to other carbonate groups analysed in this study (Table 1; Table S5). This could occur if biologic processes are a factor in influencing observed  $\Delta_{47}$ -temperature relationships and/or are a source of scatter/noise;  $r^2 = 0.5669$ . Uncertainty in the temperatures used for the regression may also affect the dataset.

Although biologically mediated carbonates and other freshwater carbonate types do not show statistically significant differences in slopes, an ANCOVA detects differences in intercept between biologically mediated carbonates and biogenic carbonates ( $p_{\text{intercept}} = 0.0047$ ) and fine-grained carbonates ( $p_{\text{intercept}} = 0.0379$ ). Significant differences in intercept are found between the regression for biologically mediated carbonates and the I-CDES calibration of Anderson et al. (2021) ( $p_{\text{intercept}} < 0.0001$ ). Within the UCLA-measured data set, different material types and prior publications exhibit agreement in slopes, but

show differences in intercept between UCLA-measured biogenic carbonates ( $p_{\text{intercept}} < 0.0001$ ) (Table S4). The reduced slope and elevated intercept for the calibration constructed using biologically mediated carbonates results in the largest difference in estimated temperatures at lower  $\Delta_{47}$  values relative to other calibrations produced in this study and the calibrations of Anderson et al. (2021) and Petersen et al. (2019).

Kato et al. (2019) found that tufa samples recorded lower  $\Delta_{47}$  values relative to synthetic calcite and application of a synthetic calcite-based regression to tufa samples resulted in temperature estimates for tufas that were higher than modern environmental temperatures. Prior studies have also found lower  $\Delta_{47}$  values for tufas and travertines (Kele et al., 2015; Kato et al., 2019); however, this study does not show a relationship consistent with  $\text{CO}_2$  degassing in the residual  $\Delta_{47}$  and  $\delta^{18}\text{O}_{\text{carbonate}}$  values relative to projected equilibrium values (Figure S3). This synthesis excludes modern tufa data from Kato et al. (2019) due to discrepancies between standard values for Carrara Marble and NBS-19 relative to values reported by Bernasconi et al. (2021) and Upadhyay et al. (2021), although their calibration falls within the 95% confidence interval of the biologically mediated calibration in this study.

#### 4.1.5 | Travertines

Travertines display the highest  $r^2$  values relative to biogenic carbonates, biologically mediated carbonates and fine-grained carbonates, which may arise if they have the least complex precipitation mechanism with little biological influence relative to the other groups. The thermal control on water temperature in most of these samples may minimise uncertainty in estimated formation temperatures and relatively low seasonality in groundwater temperatures may contribute to the high  $r^2$ . However, the alkaline nature of some springs means that it is possible for travertines to form out of equilibrium, particularly at  $\text{pH} > 10$  and at lower temperatures.

The ANCOVA tests indicate the linear regression derived from travertines does not have a statistically significant slope compared to other groups of freshwater carbonates in this study but does indicate a statistically different intercept to the regression using fine-grained carbonates ( $p_{\text{intercept}} = 0.0050$ ; Table 2). The newly derived regression on the updated I-CDES reference frame has significant differences in intercept from the calibration presented in Petersen et al. (2019) ( $p_{\text{intercept}} = 0.0354$ ); however, no significant differences in either slope or intercept were found between travertines and the Anderson et al. (2021) calibration (Table 2).

The relationship between  $\Delta_{47}$  and  $\delta^{18}\text{O}_{\text{carbonate}}$  values in travertines is significant (Supplementary Figure 2); however, the relationship between the residual  $\Delta_{47}$  and  $\delta^{18}\text{O}_{\text{carbonate}}$  values relative to the estimated equilibrium does not show any significant correlation (Figure S3). Travertine samples selected for reprojection within this analysis were close to vents to minimise kinetic fractionations, and prior analysis of these samples show no influence from water chemistry, mineralogy and precipitation rate (Kele et al., 2015).

## 4.2 | Application of material-specific and composite freshwater calibrations

### 4.2.1 | Reconstructed temperatures

Overall, an ANCOVA suggests no statistically significant difference between the calibration slopes derived from different materials and previously published calibrations (Table 2). Calibrations converge on a common temperature dependence (slope) for clumped isotope measurements when dividing freshwater carbonates into groups to account for potential differences in their precipitation (e.g., seasonality, ecology, etc.). A similar convergence of slopes was found in Petersen et al. (2019) when comparing 14 different clumped isotope studies of both biogenic and abiogenic carbonates using updated parameters for calculation of  $\Delta_{47}$  values. Anderson et al. (2021) also found a convergence of slopes between their new data, the Petersen calibration and recalculated calibration lines using updated carbonate standardisation procedures for four recent calibration studies. However, the ANCOVA analyses indicate statistically different intercepts for most calibrations from groups of freshwater carbonates (Table 2).

Figure 4A shows a comparison of residuals for temperatures calculated using calibrations derived from material-specific carbonates and composite freshwater carbonates. For temperature, a decrease in residuals occurs when utilising material-specific regressions for biogenic and fine-grained carbonate archives. In the case of travertines and biologically mediated carbonates, use of the composite freshwater calibration reduces temperature residuals relative to the material-specific calibration. The root mean square error (RMSE) evaluates goodness of fit for each of the two types of models. The RMSE shows, on average, how far away the predicted  $\Delta_{47}$ -derived values were from the measured values (both positively and negatively) and allows for intercomparison in the same units. Applying the composite freshwater calibration to biogenic samples results in a RMSE of 4.4°C, while applying the biogenic calibration results in an RMSE of 2.9°C, showing

a better fit when using the material-specific calibration. Temperatures derived from a fine-grained carbonate-specific calibration results in a slightly lower RMSE than a composite calibration (3.9 and 4.6°C, respectively).

In contrast, the composite freshwater calibration slightly outperforms the material-specific calibrations for biologically mediated carbonates and travertines, resulting in a lower RMSE than their material-specific counterparts (biologically mediated carbonates: 4.4 and 5.1°C, travertine: 6.5 and 7.1°C). For biologically mediated carbonates and travertines, the improvement in prediction quality is small when using a material-specific calibration relative to the calibration derived from all freshwater carbonates. Both calibrations overestimate formation temperature for high-temperature travertines. When excluding the two highest temperature travertine samples (95°C), both the composite and material-specific calibrations perform similarly when applied to the travertine data set (RMSE = 4.9°C for both calibrations).

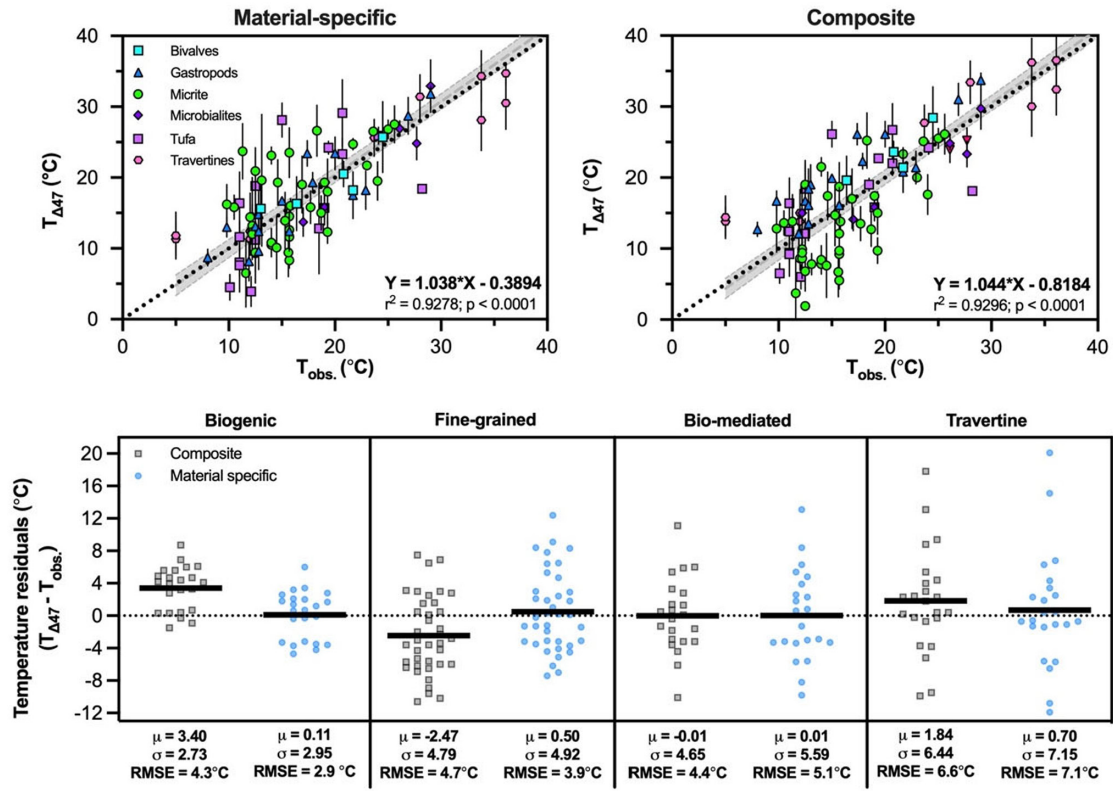
Thus, these results suggest that material-specific calibrations will yield more accurate results for biogenic and fine-grained carbonate samples, although the differences are relatively small for some sites, they are larger for others (Figure 4). A composite freshwater calibration will yield slightly more accurate results for biologically mediated carbonates and travertines.

### 4.2.2 | Reconstructed water $\delta^{18}\text{O}$ values

In addition to providing thermodynamic constraints on the temperature of formation of carbonates,  $\Delta_{47}$  measurements paired with carbonate oxygen isotope ratios can directly calculate source water  $\delta^{18}\text{O}$  values. Thus, to evaluate if this method can accurately reconstruct the isotopic composition of the water in which the carbonate precipitated, this study compares the clumped isotope derived estimates of water  $\delta^{18}\text{O}$  values derived with  $\Delta_{47}$ -temperature predictions ( $\delta^{18}\text{O}_{\text{w-reconstructed}}$ ) to directly measured modern freshwater  $\delta^{18}\text{O}$  ( $\delta^{18}\text{O}_{\text{w-measured}}$ ) values. Published  $\delta^{18}\text{O}_{\text{w-measured}}$  values are available for 86 of the 108 sites (Table S6). Although some sites had long-term measurements of water body oxygen isotope composition, some of the measurements were single point measurements, and thus may not fully represent temporal variability.

This study uses the equations of Kim and O'Neil (1997) for calcite and Kim et al. (2007) for aragonite to constrain the relationship between formation temperature,  $\delta^{18}\text{O}_{\text{carbonate}}$  and  $\delta^{18}\text{O}_{\text{water}}$  values. There is a positive relationship between measured and clumped isotope-derived  $\delta^{18}\text{O}_{\text{w-reconstructed}}$  values when using the reconstructed temperatures using both the composite freshwater calibration

### A Water temperature



### B Water $\delta^{18}O$

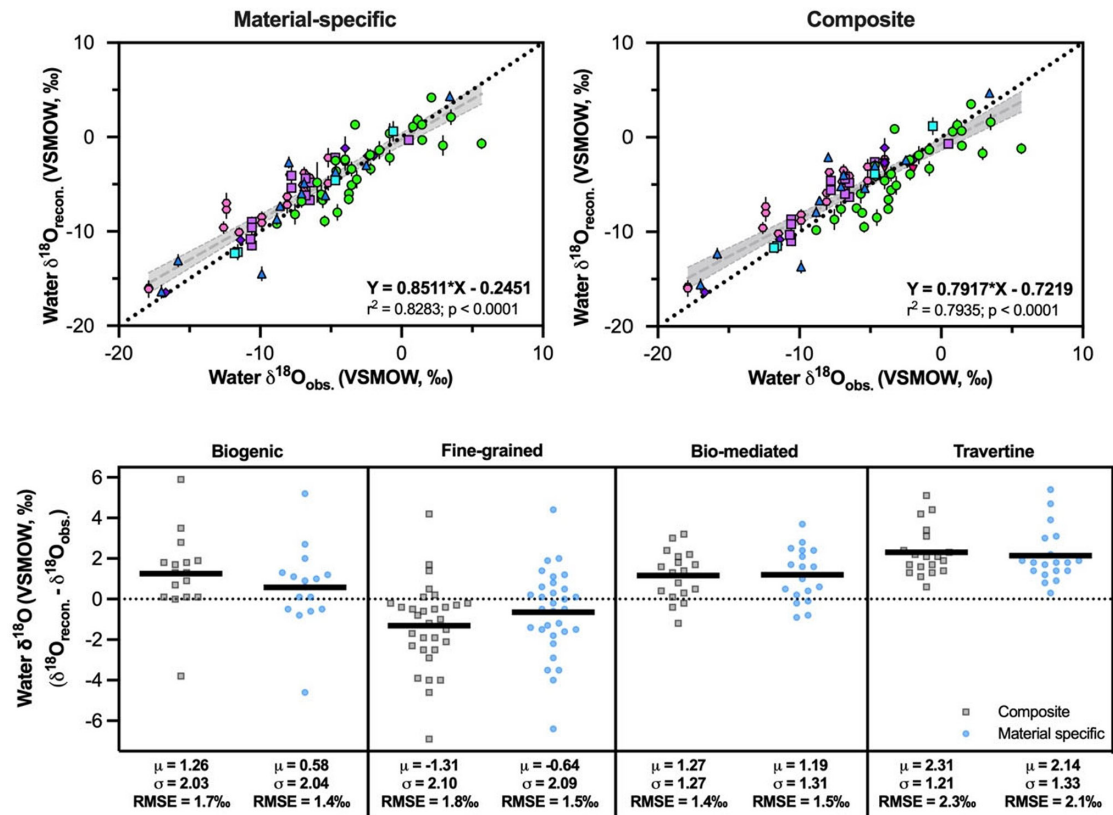


**FIGURE 4** Comparison of reconstructed values of temperature and  $\delta^{18}\text{O}_{\text{water}}$  from material-specific and composite calibrations from this study to observations. Use of a composite  $\Delta_{47}$ -temperature calibration yields less accurate and precise results. (A) Comparison of measured temperature ( $T_{\text{obs}}$ ) to  $\Delta_{47}$ -derived temperature ( $T\Delta_{47}$ ) values using the material-specific and composite freshwater calibration. Bottom panel shows a comparison of temperature residuals (reconstructed observations) using the composite and material-specific calibrations. Blue circles and black squares represent values derived using the material-specific and composite freshwater regression, respectively. Horizontal black bars represent the mean and values at the bottom of each data set show the mean value and standard deviation for residuals along with the RMSE for each data set using the respective calibrations. (B) Comparison of measured  $\delta^{18}\text{O}_{\text{water}}$  ( $\delta^{18}\text{O}_{\text{obs}}$ ) to  $\Delta_{47}$ -derived  $\delta^{18}\text{O}_{\text{water}}$  values ( $\delta^{18}\text{O}_{\text{recon}}$ ) using material-specific and composite freshwater calibration.  $\delta^{18}\text{O}_{\text{water}}$  values use  $\Delta_{47}$  temperatures calculated using either the composite or material-specific calibrations, and oxygen isotope mineral-water fractionation factors from Kim and O'Neil (1997) (calcite) or Kim et al. (2007) (aragonite). Bottom panel displays  $\delta^{18}\text{O}_{\text{water}}$  residuals (reconstructed observations) using the composite and material-specific calibrations. Generally, there is some improvement in RMSE for temperature and  $\delta^{18}\text{O}_{\text{water}}$  reconstructions for the use of material-specific calibrations, though in the case of bio-mediated carbonates and travertines, the improvement is small to negligible.

( $p < 0.0001$ ;  $r^2 = 0.7935$ ) and material-specific calibrations presented in this study ( $p < 0.0001$ ;  $r^2 = 0.8267$ ). Figure 4B shows a comparison of the residuals for reconstructed  $\delta^{18}\text{O}_{\text{w}}$  values using both the material-specific and composite calibrations developed within this study. There is a reduction in the RMSE when using the material-specific calibration relative to the composite calibration for biogenic carbonates (material-specific RMSE = 1.5‰, composite RMSE = 1.8‰), fine-grained carbonates (material-specific RMSE = 1.4‰, composite RMSE = 1.7‰) and travertines (material-specific RMSE = 2.1‰, composite RMSE = 2.3‰). However, for biologically mediated carbonates, the composite calibration slightly outperforms the material-specific calibration (material-specific RMSE = 1.4‰, composite RMSE = 1.5‰), although the mean of the residuals is closer to zero.

Overall, both the composite and material-specific calibrations perform well in reconstructing  $\delta^{18}\text{O}_{\text{w-measured}}$  values. Of the 87 samples from sites with measured  $\delta^{18}\text{O}_{\text{water}}$  values, when using temperatures derived from the material-specific and composite freshwater calibration, 33 and 27 samples, respectively, fall within  $\pm 1\%$  of hydrographic data (Figure 4B). The  $\delta^{18}\text{O}_{\text{w-reconstructed}}$  values for biogenic samples generally recover  $\delta^{18}\text{O}_{\text{w-measured}}$  values within 2‰. However, this method yields, for fine-grained carbonates, lower  $\delta^{18}\text{O}_{\text{water}}$  values than observations for more enriched  $\delta^{18}\text{O}_{\text{w-measured}}$  values, which could be due to either kinetic effects and/or changes in surface water chemistry during carbonate precipitation events (Figure 4B). If the latter, it is unlikely to be due to evaporative enrichment of  $\delta^{18}\text{O}_{\text{water}}$  values which would produce the opposite trend, but it may arise from changes in carbonate chemistry. Figure 4B shows biologically mediated carbonates and travertines show a positive offset from the 1:1 line, overestimating  $\delta^{18}\text{O}_{\text{water}}$  relative to the measured value, that may also arise from pH-related effects on isotopic fractionation or kinetic isotope effects (Beck et al., 2005; Tripathi et al., 2015).

### 4.3 | Comparison of multiple materials at individual sites

Five lakes contain two different types of freshwater carbonates analysed in this study. Three sites in China (Daija Co, Cuona Lake and Wulungu Lake) contain both fine-grained carbonate (Li et al., 2021) and freshwater molluscs (this study). Two locations in the Great Salt Lake (North Arm and South Arm, which are restricted by a causeway and chemically unique; Pace et al., 2016) contain microbialites and ooids. Comparing water temperature estimates from different carbonate types provides another method of assessing overall calibration performance. Therefore, this study compares clumped isotope-derived temperatures using both material-specific and composite freshwater calibrations at sites where different materials are present and considered in light of current knowledge about the seasonality of carbonate formation.

Figure 5 shows increased agreement between different sample types for the same location for temperature and water  $\delta^{18}\text{O}$  values in a majority of cases with the use of a material-specific calibration. If the model derived in this study was perfect, samples should follow the 1:1 line (denoted by grey dashes in Figure 5), where the reconstructed temperatures and water  $\delta^{18}\text{O}$  values match the observations. In the case of water temperature, applying the material-specific calibration derives a slope and intercept pair closer to the 1:1 line in comparison to the composite calibration. Additionally, estimates of water temperature using material-specific calibrations exhibit increased correlation between samples, with  $r^2$  values of 0.846 and 0.798 when applying the material-specific and composite calibrations, respectively. For water  $\delta^{18}\text{O}$  values, similar positive slopes that are slightly greater than 1 are calculated between the reconstructed and measured values for both calibrations (slope<sub>material specific</sub> = 1.304, slope<sub>composite</sub> = 1.249), but increased correlation between the samples when applying the material-specific calibrations.

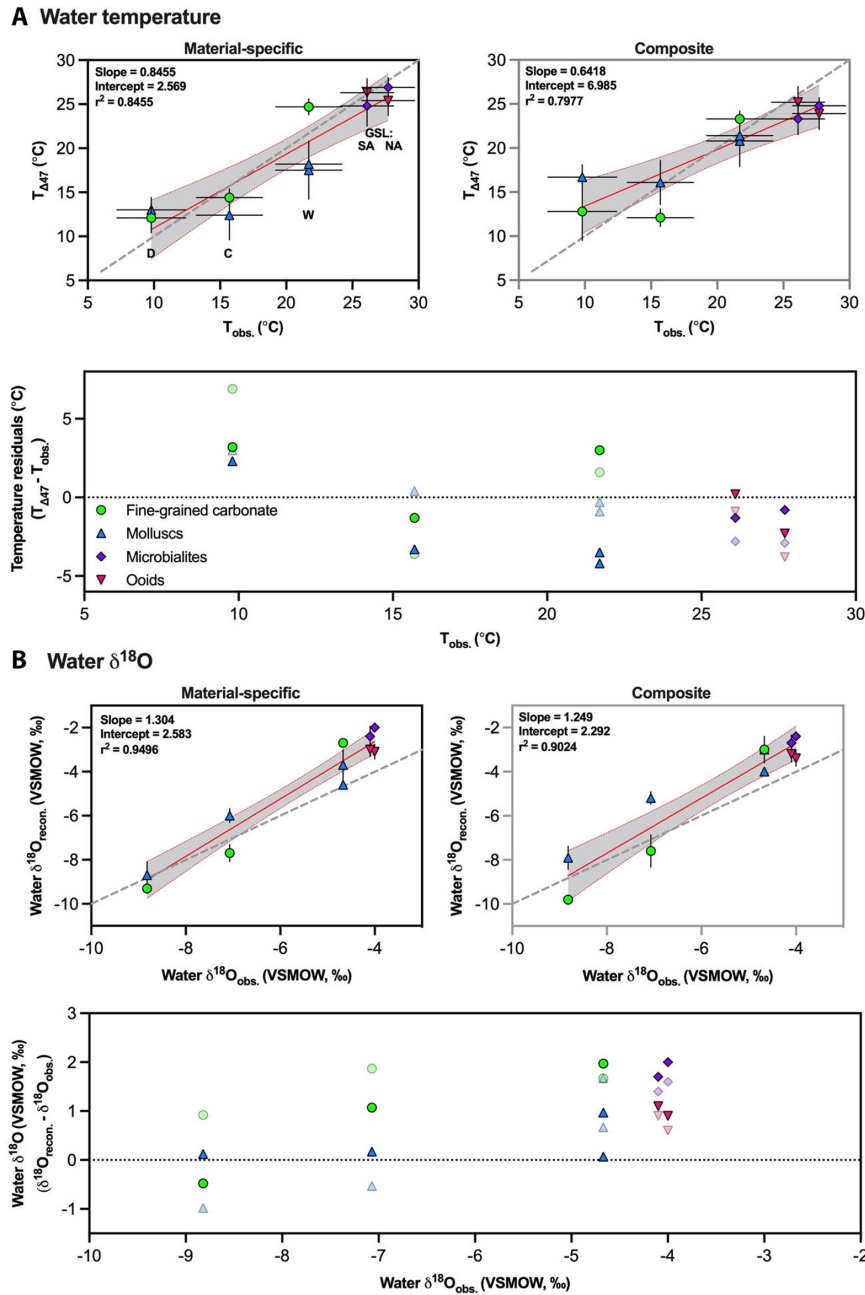


**FIGURE 5** Evaluation of clumped isotope-derived temperature and  $\delta^{18}\text{O}_{\text{water}}$  for locations with dual materials. (A) Clumped isotope-derived temperature reconstructions using material-specific calibrations (top row; black frame) and composite freshwater calibration (top row; grey frame). Red lines and grey shading show the linear regression and the 95% confidence interval through the data, respectively. Bottom panel shows residuals for both the material-specific calibrations and composite calibrations (semi-transparent symbols), along with the average difference in temperature between the two archives (black and grey numbers and lines for material-specific and composite calibration, respectively).  $T_{\Delta 47}$  represents temperatures derived from clumped isotope analysis, while  $T_{\text{obs}}$  represents independently observed water temperatures. Sites are labelled on plot: D: Daija Co, C: Cuona Lake, W: Wulungu Lake, GSL NA: North Arm, Great Salt Lake, GSL SA: South Arm, Great Salt Lake. Using a material-specific calibration results in a reduction of temperature residuals in most cases. Material-specific calibrations also yield more realistic temperature estimates, given each lake's individual setting. (B) Reconstructed water  $\delta^{18}\text{O}$  values using material-specific (top row, black frame) and composite (top row, grey frame) calibrations. Water  $\delta^{18}\text{O}_{\text{recon}}$  and water  $\delta^{18}\text{O}_{\text{obs}}$  represent clumped isotope-based reconstructions of water  $\delta^{18}\text{O}$  and independently measured values of water  $\delta^{18}\text{O}$ , respectively. Red lines and grey shading show the linear regression and the 95% confidence interval through the data, respectively. The bottom plot displays the residuals from the measured values, with black and grey bars for the material-specific and composite calibrations, respectively.



All three lakes in China examined in this section are terminal lakes where authigenic carbonate precipitation is likely to occur in the later part of summer, when temperatures are most elevated and carbonate supersaturation occurs in the surface waters (Hren & Sheldon, 2012). Both Daija Co and Cuona Lake are high elevation lakes (>4.5 km) where the monthly average air temperature does not exceed 0°C until May; thus, temperature requirements for mollusc calcification and growth are met during similar times of year, as are the conditions necessary for the generation of authigenic carbonate. As expected, both archives produce similar estimated temperatures when using the material-specific calibrations. However, applying the composite calibration to samples in these lakes results in a disparity between calcification temperatures projected for both types of carbonates, with molluscs estimating higher water temperatures relative to the authigenic carbonate. In contrast to the setting of Daija Co and Cuona Lake, Wulungu Lake is an inland, low elevation and high latitude (47°N) lake with a large range of intra-annual air temperatures (*ca* 36°C). The large intra-annual air temperature range would likely extend to lake water temperatures. Authigenic carbonates are more likely to have temperature-induced precipitation and evaporative enrichment here; results using a material specific calibration suggest that fine-grained carbonate precipitated during a narrower interval, with higher temperatures and  $\delta^{18}\text{O}$  values than the mollusc samples at the same sites. The water temperatures recorded by molluscs at the same lake using the material-specific calibrations suggest that the shells may be reflecting dominant calcification during comparatively cooler temperatures in spring or early summer. This is consistent with prior work showing that some molluscs have a species-dependent threshold of water temperatures that allows for calcification and survival (Versteegh et al., 2010); thus, the disparity between the two archives may show that the thermal maxima of lake water temperatures may inhibit mollusc calcification.

Pairs of carbonate material were also collected from locations in each arm of the Great Salt Lake and analysed in this study. The separation of the North and South arms of the Great Salt Lake by a causeway result in a more restricted Northern arm with less freshwater input from rivers, higher water temperatures and salinity, lower pH and more evaporation (Gwynn, 2007; Ingalls et al., 2020). Ooids from the Great Salt Lake have been found to form concentrically throughout the past 6600 years (Paradis, 2019). Recent work suggests that Great Salt Lake ooids are insensitive to short-term changes in lake conditions and/or biologically induced changes within the lake, and their isotopic composition has been shown to represent time-averaged conditions, while microbialites from the Great Salt Lake have been shown to record  $\delta^{18}\text{O}_{\text{carb}}$

and  $\Delta_{47}$  values in equilibrium with lake water  $\delta^{18}\text{O}$  values (Ingalls et al., 2020). Despite the longer timescale of carbonate precipitation between ooids and microbialites, prior work shows consistency between clumped isotope-derived reconstructions of temperatures of both carbonate types (Ingalls et al., 2020). Thus, both materials can be used to reconstruct modern temperatures and evaluate calibration performance for dual material archives.

The  $\Delta_{47}$ -derived temperature reconstructions derived from microbialites show elevated heating in the North Arm relative to the South Arm using both the material-specific (2.1°C) and composite calibrations (1.5°C), with a similar extent as modern lake water temperature measurements from each site (1.5°C). Reconstructions from ooids fail to capture the modern temperature gradient observed between arms of the lake but are within error of each other and modern summer water temperatures. This disparity between microbialites and ooids is likely due to the differences in timescale of carbonate formation between archives. It is unlikely that the ooid composition reflects short-term changes in the two arms due to the separation from the causeway given the longer relative timescale of ooid formation.

Temperatures derived using material-specific calibrations have increased agreement between modern water temperatures in both arms of the lake (Figure 5). The use of the composite freshwater calibration generally underestimates formation temperatures relative to modern water temperature measurements. Further study is necessary to fully understand the differences in calcification between archives in the same settings, but these findings may support the use of a material-specific calibration when developing reconstructions from multiple types of carbonates for ancient freshwater systems.

## 4.4 | Applications to Palaeoclimate Reconstructions

### 4.4.1 | Origin of travertine and tufa deposits in Ainet, Austria

Application of the material-specific and composite freshwater calibrations constructed in this study examines the origins of late glacial sequences of travertine and calcareous tufa from Ainet, Austria, that was first described in Boch et al. (2005). This sequence of *ca* 2.7 m thickness formed over the course of *ca* 1000 years, following the rapid initiation of warming during the Bølling-Allerød, and represents the only aragonitic travertine sequence known in the Eastern Alps (Figure 6). Carbonate deposition within the travertine sequence alternated between aragonite and calcite layers (on millimetre-scale). Previous

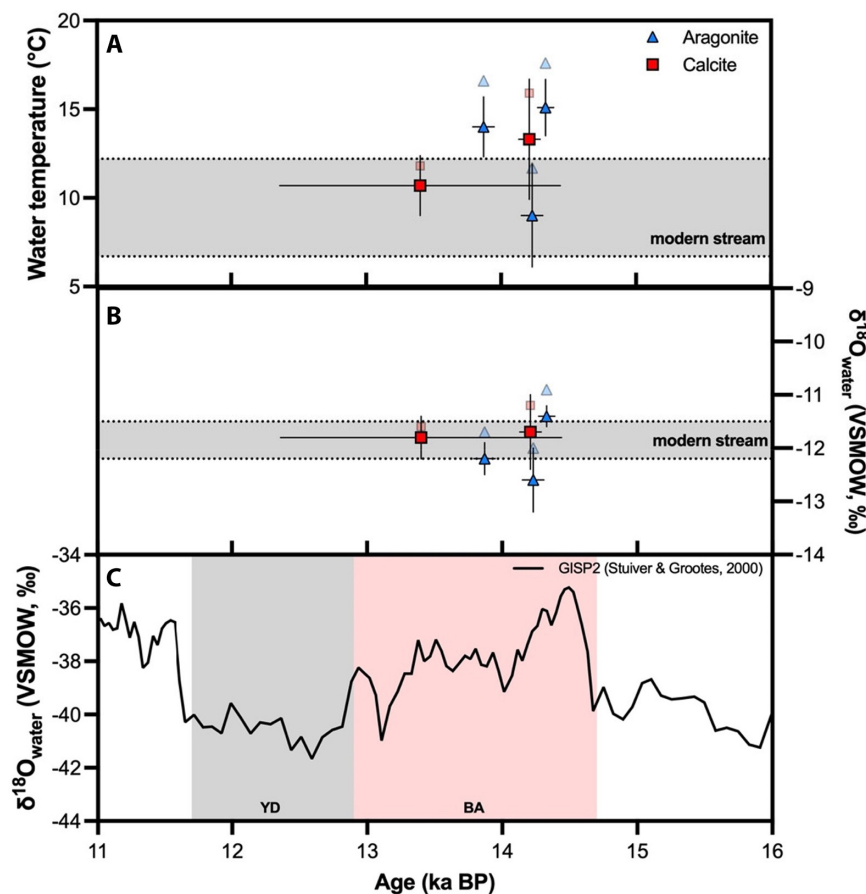


**FIGURE 6** Clumped isotope-derived estimates of (A) temperature and (B)  $\delta^{18}\text{O}_{\text{water}}$  for a travertine terrace in Ainet, Austria. Solid symbols represent estimates derived from material-specific calibrations, while lighter symbols represent estimates derived from the composite freshwater calibration. Grey bands represent the range of modern stream values measured in May, July and October (Boch et al., 2005) and (C) data for GISP2 ice core record are from Stuiver and Grootes (2000). Values are broadly consistent with modern temperatures and  $\delta^{18}\text{O}_{\text{water}}$  of nearby streams.

work proposed that the alternating mineralogy represents differences in seasonality, with aragonite and calcite precipitation occurring during the warm and cool seasons, respectively (Boch et al., 2005). A calcareous tufa layer (*ca* 0.2 m) consisting solely of calcite caps the sequence of the compact and aragonite-dominated travertine (*ca* 2.5 m).

Temperature estimates derived using material-specific calibrations for the tufa and travertine sequence range from 9.0 to 15.1°C, with an average value of 12.7°C for the travertine terrace (Table S7). Modern water temperatures taken in May, July and October range from 6.6 to 12.2°C, similar to the  $\Delta_{47}$ -derived estimates. A clear relationship between temperature and mineralogy is not apparent within this limited data set, despite the initial study suggesting a seasonal control on aragonite and calcite formation, with aragonite and calcite precipitation occurring in the warmer and cooler months, respectively (Figure 6).

The  $\Delta_{47}$ -temperatures and  $\delta^{18}\text{O}_{\text{water}}$  values support the hypothesis that the travertine sequence did not have a hydrothermal origin (thermal water discharge), but are consistent with being derived from rapid  $\text{CO}_2$  degassing from groundwater discharge of meteoric origin, with sufficient time for dissolved inorganic carbon (DIC) equilibration to occur. Modern  $\delta^{18}\text{O}_{\text{water}}$  values measured from

a series of nearby streams ( $-11.5$  to  $-12.1$ ‰ VSMOW) are consistent with  $\delta^{18}\text{O}_{\text{water}}$  estimates derived from clumped isotope analysis ( $-11.4$  to  $-12.2$ ‰ VSMOW). Given this consistency in  $\delta^{18}\text{O}_{\text{water}}$ , these results suggest recharged meteoric groundwater (seasonal rainfall, snowmelt) and eventually some contribution from ice melting due to a rapid increase in temperatures during the Bølling-Allerød is likely to have been the surface-dominated palaeofluid source for carbonate precipitation here.

The analysis of this travertine sequence illustrates the importance of an appropriate calibration selection. While application of the composite freshwater carbonate calibration would yield temperature values 2.5–2.7°C higher than modern streamflow, use of the material-specific calibrations yields formation temperatures more similar to modern stream temperatures (Table S7), which are more likely to be correct for carbonates forming in an interval of distinct relative warmth in the last glacial period. The  $\delta^{18}\text{O}_{\text{water}}$  values reconstructed from the material-specific calibration are within error of modern groundwater values, measured from spring-fed streams, while reconstructed  $\delta^{18}\text{O}_{\text{water}}$  values are 0.5–0.6‰ higher when using the composite calibration relative to the material-specific calibration.

#### 4.4.2 | Palaeoclimatology of Lake Surprise, CA

Santi et al. (2020) reconstructed hydroclimate at Lake Surprise, California, by applying clumped isotope thermometry to reconstruct terrestrial palaeo-hydroclimate variables using samples of tufa from the last glacial maximum (LGM; 23,000–19,000 years ago) and deglacial (19,000–11,000 years ago) (Egger et al., 2018; Ibarra et al., 2014; Santi et al., 2019, 2020). In Ibarra et al. (2014), the authors used an isotope mass balance model to derive evaporation and precipitation rates by using pollen data to constrain the temperature changes within their model. Santi et al. (2020) expanded on this work by providing further clumped isotope-derived constraints on water temperatures and  $\delta^{18}\text{O}_{\text{water}}$  values for the same sample set and used these updated values within a revised modelling framework to derive new estimates of evaporation and precipitation rates. This study utilises the data set presented in Santi et al. (2020) to evaluate the consequences of calibration choice on temperature and water  $\delta^{18}\text{O}$  estimates and provide a first order estimate of how changes in these values would modify clumped isotope-derived hydroclimate variables, including water temperature,  $\delta^{18}\text{O}_{\text{water}}$  values, mean annual air temperature (MAAT), evaporation rates and precipitation rates. Data are shown in the I-CDES reference frame following current best practices

and standardisation procedures (Bernasconi et al., 2021; Upadhyay et al., 2021).

Table 3 shows the impact of applying different calibrations on water temperature and  $\delta^{18}\text{O}_{\text{water}}$  values to the Lake Surprise data set for LGM and deglacial samples, relative to the original publication (see Figure S5). Tables S8 and S9 show the results from utilising different calibrations on hydroclimate parameter estimates. On first order, the composite calibration derived from all freshwater carbonates generally produces 0.8°C warmer water temperatures and 0.2‰ higher  $\delta^{18}\text{O}_{\text{water}}$  values than the original publication (Table 3). This results in a similar pattern in MAAT, with 0.9–1.1°C increases in MAAT, and overall increases in evaporation rates of 90–122 mm/year. and precipitation rates of 36–40 mm/year. relative to the estimates calculated from the original publication values (Figure S5). Water temperatures and  $\delta^{18}\text{O}_{\text{water}}$  estimates derived using the material-specific calibration for biologically mediated carbonates are about 1°C cooler and 0.3‰ lower than the values estimated from the freshwater composite calibration, with similar evaporation rates (ranging from 11 mm/year decreases and 60 mm/year increases relative estimates derived from the original publication) and precipitation rates (ranging from 15 mm/year increases and 0 mm/year increases relative to estimates derived from the original publication; Table 3), and are relatively similar to values in the original publication. In contrast, applying the calibration from Anderson

**TABLE 3** Comparison of recalculated  $\Delta_{47}$ -based reconstructions derived from the material-specific, composite freshwater and calibration from Anderson et al. (2021) to published values. Top: Comparison of water temperature and water  $\delta^{18}\text{O}$  at Lake Surprise, CA to published values from Santi et al. (2020). Bottom: Comparison of clumped isotope-derived water temperature and water  $\delta^{18}\text{O}$  for samples run for clumped isotope analysis from the Nangqian Basin to published values from Li et al. (2019).

Hydroclimate reconstruction at Lake Surprise, CA						
(41.5°N, 120.0° W)	$T_w$ (°C)		$\delta^{18}\text{O}$ (‰)			
	LGM	Deglacial	LGM	Deglacial		
This study—material-specific	11.2 ± 6.7	10.5 ± 4.4	−4.0 ± 2.0	−4.1 ± 1.4		
This study—composite	12.1 ± 5.4	11.6 ± 3.6	−3.8 ± 1.6	−3.8 ± 1.2		
Anderson et al. (2021)	9.6 ± 6.0	9.0 ± 4.0	−4.4 ± 1.2	−4.3 ± 1.6		
Santi et al. (2020)	11.3 ± 4.5	10.8 ± 3.0	−4.0 ± 1.3	−4.0 ± 1.0		
Elevation reconstruction in Nangqian Basin, Tibetan Plateau						
(32.2°N, 96.5°E)	Unit 1 (mid Cretaceous)		Unit 3 (mid Palaeogene; >38 Ma)		Unit 4 (38–37 Ma)	
	$T_w$ (°C)	$\delta^{18}\text{O}_w$ (‰)	$T_w$ (°C)	$\delta^{18}\text{O}_w$ (‰)	$T_w$ (°C)	$\delta^{18}\text{O}_w$ (‰)
This study—material-specific	25.1 ± 3.0	−6.0 ± 1.2	39.0 ± 3.7	−5.0 ± 0.8	30.3 ± 3.5	−6.2 ± 1.1
This study—composite	23.7 ± 3.3	−6.3 ± 1.0	38.8 ± 4.1	−5.0 ± 0.7	27.9 ± 3.8	−6.5 ± 1.0
Anderson et al. (2021)	21.7 ± 3.4	−6.7 ± 1.0	37.7 ± 4.4	−5.2 ± 0.8	26.1 ± 4.0	−6.8 ± 1.0
Li et al. (2019)	24.9 ± 2.8	−6.2 ± 1.5	40.9 ± 4.1	−4.6 ± 0.9	29.7 ± 3.7	−6.2 ± 1.4

et al. (2021) results in 1.8°C cooler temperatures and 0.4‰ lower  $\delta^{18}\text{O}_{\text{water}}$  values relative to the original results, a similar offset from material-specific estimates, and 1.4–1.5°C cooler temperatures than the freshwater composite calibration. The reduction in water temperatures relative to the other calibrations results in MAAT estimates for the deglacial that are 2.5–2.9°C cooler than the original publication, and subsequent reductions in evaporation (139–180 mm/year) and precipitation rates (73–95 mm/year) (see Text S1).

#### 4.4.3 | Palaeoaltimetry of the Tibetan Plateau

Clumped isotope-derived constraints on water temperature and water  $\delta^{18}\text{O}$  values can aid in constraining the evolution of the tectonic and topographic history of a region (Ghosh et al., 2006a; Quade et al., 2013; Huntington & Lechler, 2015; Li et al., 2019; Richter et al., 2022). This proxy relies on the premise that lake water temperature is directly related to air temperature; therefore, as basins undergo surface uplift as a result of large-scale tectonic processes (e.g., crustal shortening and thickening, convective removal of lower lithosphere, etc.), the ambient air and water temperature should decrease, as governed by the local lapse rate (Ghosh et al., 2006a; Quade et al., 2013; Huntington & Lechler, 2015; Li et al., 2019). Reconstructed  $\delta^{18}\text{O}_{\text{water}}$  values can provide additional constraints on palaeoelevation, because the stable isotope compositions of meteoric and surface waters decreases as altitude increases (Chamberlain & Poage, 2000; Poage & Chamberlain, 2001; Rowley & Garzzone, 2007).

This study assesses the impact of calibration choice (the composite freshwater carbonate and material-specific calibration from fine-grained carbonates) using a published palaeoelevation reconstruction of the Nangqian Basin, located in the east-central Tibetan Plateau, from Li et al. (2019). Table 3 shows water temperatures and  $\delta^{18}\text{O}_{\text{water}}$  values for lacustrine samples spanning the Late Cretaceous to the Late Eocene using each calibration.

Mean temperatures for the Late Cretaceous through late Eocene derived using the material-specific calibration are within 0.2 and 1.9°C of the published results, while the composite freshwater calibration results in 0.2–1.4°C lower temperatures (Table S10). Applying the calibration of Anderson et al. (2021) results in even cooler temperatures for each unit than the equations derived in this study, ranging from 3.2 to 3.6°C lower than the original publication. The  $\delta^{18}\text{O}_{\text{water}}$  values (Table S10) show a similar pattern.

Additionally, this study uses the clumped isotope-derived results to compare estimates of elevation changes during the late Eocene (38–37 Ma) following the two approaches used in Li et al. (2019). In the first approach, a model that partitions dominant regional moisture sources

uses Late Eocene  $\delta^{18}\text{O}_{\text{water}}$  values to estimate palaeoelevation (Li et al., 2019). Using a material-specific calibration results in  $\delta^{18}\text{O}_{\text{water}}$  estimates that support a mean hypsometric palaeoelevation of  $2.8 \pm 1.1$  km and  $3.1 \pm 1.1$  km, similar to the original reconstruction ( $2.8 \pm 1.1$  km and  $3.2 \pm 1.1$  km), and *ca* 1.3 km lower than the modern hypsometric mean elevation (4.2 km) of the Nangqian Basin. The cooler temperatures derived using the calibration of Anderson et al. (2021) result in more depleted water  $\delta^{18}\text{O}$  values and similar estimates of palaeoelevation ( $2.9 \pm 1.1$  km and  $3.2 \pm 1.1$  km), but still within error of the original publication and the material-specific calibration.

Second, the authors use clumped isotope-derived estimates of water temperature and a lapse rate that relates elevation to modern lake water temperatures on the Tibetan Plateau. The material-specific calibration using Late Eocene fine-grained carbonates results in a mean  $T-\Delta_{47}$  value of carbonates of 30.3°C, 0.3°C higher than the published value. This mean  $T-\Delta_{47}$  value is 13.3°C higher than the estimated modern warm-season lake surface water temperature (*ca* 17°C) at 3.8 km. Post-Eocene global cooling accounts for roughly 6°C of the temperature decrease (Hansen et al., 2008), while the remaining temperature decrease (6.5°C) would reflect palaeoelevation increases of the basin floor after the Eocene. Applying a lapse rate of  $-6.1 \pm 1.0^\circ\text{C}/\text{km}$  for lake surface water temperature on the Tibetan Plateau (Huntington et al., 2015) results in  $1.0 \pm 0.3$  km of post-Late Eocene elevation increase and palaeoelevation estimates of 2.8 km for the basin floor when applying a material-specific calibration.

Late-Eocene lake water temperatures estimated from the freshwater composite calibration are 10.9°C higher than modern warm season values, resulting in elevation change estimates of 0.8 km elevation increase. The cooler temperatures estimated from composite freshwater calibration result in palaeoelevation estimates of 3.0 km above sea level for the Nangqian Basin during this time. The Anderson et al. (2021) calibration estimates lake water temperatures are 9.1°C warmer than modern warm season values. The reduction in estimated water temperatures relative to the other calibration results in a palaeoelevation estimate for the basin floor of 3.3 km above sea level, with 0.5 km of uplift occurring post Late-Eocene. The palaeoelevation estimates derived from Anderson et al. (2021) are 0.5 km lower than those derived using a material-specific calibration.

## 5 | CONCLUSIONS

In order to confidently use proxies to characterise and understand past environments, it is necessary to have a solid understanding of modern systems. This work

presents an extensive composite data set of 135 clumped isotope samples of terrestrial freshwater carbonates from 96 sites and derives relationships between modern water temperatures and  $\Delta_{47}$  values. These freshwater  $\Delta_{47}$ -temperature calibrations are well constrained, encompass a variety of types of natural lacustrine, fluvial and spring carbonates, and span a broad range of temperatures, elevations and latitudes. As all carbonates in this study are from modern freshwater settings, they are more representative of real-world systems, and may, in some circumstances, be more appropriate for application to reconstruct palaeotemperatures, than  $\Delta_{47}$ -temperature carbonate calibrations from experimentally grown carbonates. However, since this approach utilises in situ lake water surface temperature data, there is an added uncertainty in the timing of carbonate formation temperature and calcification timeframe for each of the calibration samples. Additionally, for some freshwater carbonates, the material-specific calibrations are still relatively limited in size (minimum  $n = 22$ ). This study recommends the application of material-specific calibrations for samples that fall within the range of calibration development, with limits on the extrapolation far outside of the range.

The results of this study show a convergence of slopes but differences in the intercepts of the  $\Delta_{47}$ -temperature relationship between freshwater carbonate groups. Specifically, an ANCOVA analysis shows that material-specific calibrations based on grouping freshwater carbonates (biogenic, biologically mediated, fine-grained carbonate and travertine) have statistically indistinguishable slopes between other freshwater carbonate groups and recently published calibration studies, but in some cases, where there is strong evidence for a biogenic origin, detects differences in intercepts. In many cases, implementing material-specific calibrations reduces the magnitude of residuals (offsets between  $\Delta_{47}$ -derived temperatures/water  $\delta^{18}\text{O}$  and measured temperature/water  $\delta^{18}\text{O}$ ) and RMSE. However, the calculated values from the composite and material-specific freshwater calibrations are often within 1.0–1.5°C of each other, indicating generally good agreement. Water  $\delta^{18}\text{O}$  values derived from utilising material-specific calibrations can recover independently measured water  $\delta^{18}\text{O}$  values with reasonable accuracy, with 39 and 74% of lakes being within 1 and 2‰ of measured water  $\delta^{18}\text{O}$  values, respectively, reflecting a 7 and 10% improvement relative to the composite freshwater calibration. Seasonal formation biases and/or differential expressions of kinetic effects that are not well constrained may explain the relatively small variations in different archives.

Additionally, this study examines three terrestrial palaeoreconstructions using  $\Delta_{47}$  measurements of

freshwater carbonates to evaluate the impact of different calibration relationships. First, a new data set from a travertine sequence in Austria shows that material-specific calibrations yield the most reasonable estimates. This study hypothesises that this deposit was likely derived from groundwater sources due to increased percolation of meteoric water and glacial melt. Second, hydroclimate parameters using a recalculation of temperatures with the biologically mediated and composite freshwater calibrations at Lake Surprise show small differences in reconstructions. Third, Eocene palaeoelevation estimates of the Nangqian Basin within the Tibetan Plateau using the fine-grained carbonate calibration suggest that the material-specific calibration-derived elevations are in agreement with the original publication, and that elevations derived using the composite freshwater calibration suggest 300 m higher uplift, which is not enough to change the conclusions of the paper. Overall, this work provides a basis for more accurate reconstructions of terrestrial palaeoclimate, palaeohydrology and palaeoaltimetry using freshwater archives, and opens the door to more robust understandings of palaeoenvironmental processes.

## AFFILIATIONS

<sup>1</sup>Department of Atmospheric and Oceanic Sciences, University of California, Los Angeles, Los Angeles, California, USA

<sup>2</sup>Center for Diverse Leadership in Science, University of California, Los Angeles, Los Angeles, California, USA

<sup>3</sup>Department of Earth, Planetary, and Space Sciences, University of California, Los Angeles, Los Angeles, California, USA

<sup>4</sup>Institute of the Environment and Sustainability, University of California, Los Angeles, Los Angeles, California, USA

<sup>5</sup>College of Resource Environment & Tourism, Capital Normal University, Beijing, China

<sup>6</sup>Environmental Studies Program, University of Southern California, Los Angeles, Los Angeles, California, USA

<sup>7</sup>Pacific Northwest National Laboratory, Richland, Washington, USA

<sup>8</sup>Institut für Angewandte Geowissenschaften, Technische Universität Graz, Graz, Austria

<sup>9</sup>Earth, Environmental, and Planetary Sciences, Brown University, Providence, Rhode Island, USA

<sup>10</sup>Department of Geosciences, University of Arizona, Tucson, Arizona, USA

<sup>11</sup>Department of Earth and Environmental Sciences, University of Texas at Arlington, Arlington, Texas, USA

<sup>12</sup>School of Earth and Sustainability, Northern Arizona University, Flagstaff, Arizona, USA

<sup>13</sup>Department of Earth System Science, Stanford University, Stanford, California, USA

<sup>14</sup>University of Brest, Brest, France

<sup>15</sup>Laboratoire Géosciences Océan, Institut Universitaire Européen de la Mer, Brest, France

<sup>16</sup>Instituto de Geología, Ciudad Universitaria, Universidad Nacional Autónoma de México (UNAM), Ciudad de México, Mexico

<sup>17</sup>Key Laboratory of Marine Geology and Environment, Institute of Oceanology, Chinese Academy of Sciences, Qingdao, China

<sup>18</sup>School of Earth Sciences, School of Geographical Sciences, University of Bristol, Bristol, UK

## ACKNOWLEDGEMENTS

We thank Jack Oviatt for samples he helped to collect in Utah and contributed towards this manuscript. R. Boch thanks Christoph Spötl and Jürgen M. Reitner for their contribution during fieldwork and sampling related to the travertine/tufa in Austria. We thank the reviewers and editor for their handling of the manuscript.

## FUNDING INFORMATION

This work and all UCLA participants were supported by an NSF CAREER award EAR-1352212 and NSF ICER-1936715 and Heising-Simons Foundation 2021-3137, with mass spectrometry supported by the Department of Energy through BES grant DE-FG02-13ER16402, to Aradhna Tripathi. Aradhna Tripathi was also supported by a Royal Society Wolfson Visiting Fellowship. Alexandra Arnold and Lauren Santi received support from the Center for Diverse Leadership in Science which is supported by the Silicon Valley Community Foundation, Waverley Street Foundation, Packard Foundation and Sloan Foundation, and Alexandra Arnold was also supported by a Cota-Robles Fellowship. Victoria Petryshyn collected samples from the Great Salt Lake and Walker Lake as part of the International Geobiology Course, which was supported by the Agouron Foundation and the Gordon and Betty Moore Foundation. Xingqui Liu was supported by the National Natural Science Foundation of China (NSFC 41572338).

## CONFLICT OF INTEREST STATEMENT

The authors have no conflict of interest to declare.

## DATA AVAILABILITY STATEMENT

Data will be available in the Earth-Chem database, pending acceptance of the manuscript. Sample and replicate level data for restandardised samples will also be archived in the Earth-Chem database as well as the NCDC Palaeoclimatology Database.

## ORCID

Alexandra Arnold  <https://orcid.org/0000-0001-6287-8458>

## REFERENCES

- Anderson, N.T., Kelson, J.R., Kele, S., Daëron, M., Bonifacie, M., Horita, J., Mackey, T.J., John, C.M., Kluge, T., Petschnig, P., Jost, A.B., Huntington, K.W., Bernasconi, S.M. & Bergmann, K.D. (2021) A Unified clumped isotope thermometer calibration (0.5–1,100°C) using carbonate-based standardization. *Geophysical Research Letters*, 48(7), e2020GL092069. <https://doi.org/10.1029/2020GL092069>
- Aravena, R., Warner, B.G., MacDonald, G.M. & Hanf, K.I. (1992) Carbon isotope composition of lake sediments in relation to lake productivity and radiocarbon dating. *Quaternary Research*, 37(3), 333–345. [https://doi.org/10.1016/0033-5894\(92\)90071-P](https://doi.org/10.1016/0033-5894(92)90071-P)
- Arenas-Abad, C., Vázquez-Urbez, M., Pardo-Tirapu, G. & Sancho-Marcén, C. (2010) Fluvial and associated carbonate deposits. *Developments in Sedimentology*, 61, 133–175. [https://doi.org/10.1016/S0070-4571\(09\)06103-2](https://doi.org/10.1016/S0070-4571(09)06103-2)
- Beck, W.C., Grossman, E.L. & Morse, J.W. (2005) Experimental studies of oxygen isotope fractionation in the carbonic acid system at 15, 25, and 40°C. *Geochimica et Cosmochimica Acta*, 69(14), 3493–3503. <https://doi.org/10.1016/j.gca.2005.02.003>
- Bernasconi, S.M., Daëron, M., Bergmann, K.D., Bonifacie, M., Meckler, A.N., Affek, H.P., Anderson, N., Bajnai, D., Barkan, E., Beverly, E., Blamart, D., Burgener, L., Calmels, D., Chaduteau, C., Clog, M., Davidheiser-Kroll, B., Davies, A., Dux, F., Eiler, J., Elliott, B., Fetrow, A.C., Fiebig, J., Goldberg, S., Hermoso, M., Huntington, K.W., Hyland, E., Ingalls, M., Jaggi, M., John, C.M., Jost, A.B., Katz, S., Kelson, J., Kluge, T., Kocken, I.J., Laskar, A., Leutert, T.J., Liang, D., Lucarelli, J., Mackey, T.J., Mangenot, X., Meinicke, N., Modestou, S.E., Müller, I.A., Murray, S., Neary, A., Packard, N., Passey, B.H., Pelletier, E., Petersen, S., Piasecki, A., Schauer, A., Snell, K.E., Swart, P.K., Tripathi, A., Upadhyay, D., Vennemann, T., Winkelstern, I., Yarian, D., Yoshida, N., Zhang, N. & Ziegler, M. (2021) InterCarb: a community effort to improve interlaboratory standardization of the carbonate clumped isotope thermometer using carbonate standards. *Geochemistry, Geophysics, Geosystems*, 22(5), e2020GC009588. <https://doi.org/10.1029/2020GC009588>
- Bernasconi, S.M., Müller, I.A., Bergmann, K.D., Breitenbach, S.F.M., Fernandez, A., Hodell, D.A., Jaggi, M., Meckler, A.N., Millan, I. & Ziegler, M. (2018) Reducing uncertainties in carbonate clumped isotope analysis through consistent carbonate-based standardization. *Geochemistry, Geophysics, Geosystems*, 19(9), 2895–2914. <https://doi.org/10.1029/2017GC007385>
- Boch, R., Spötl, C., Reitner, J.M. & Kramers, J. (2005) A lateglacial travertine deposit in Eastern Tyrol (Austria). *Austrian Journal of Earth Sciences*, 98, 78–91.
- Boch, R., Wang, X., Kluge, T., Leis, A., Lin, K., Pluch, H., Mittermayr, F., Baldermann, A., Boettcher, M.E. & Dietzel, M. (2019) Aragonite–calcite veins of the ‘Erzberg’ iron ore deposit (Austria): environmental implications from young fractures. *Sedimentology*, 66(2), 604–635. <https://doi.org/10.1111/sed.12500>
- Brenner, M., Whitmore, T.J., Curtis, J.H., Hodell, D.A. & Schelske, C.L. (1999) Stable isotope ( $\delta^{13}\text{C}$  and  $\delta^{15}\text{N}$ ) signatures of sedimented organic matter as indicators of historic lake trophic state. *Journal of Paleolimnology*, 22(2), 205–221. <https://doi.org/10.1023/A:1008078222806>
- Chamberlain, C.P. & Poage, M.A. (2000) Reconstructing the paleotopography of mountain belts from the isotopic composition of authigenic minerals. *Geology*, 28(2), 115–118. [https://doi.org/10.1130/0091-7613\(2000\)28<115:RTPOMB>2.0.CO;2](https://doi.org/10.1130/0091-7613(2000)28<115:RTPOMB>2.0.CO;2)
- Cheng, F., Garzzone, C., Li, X., Salzmann, U., Schwarz, F., Haywood, A.M., Tindall, J., Nie, J., Li, L. & Wang, L. (2022) Alpine permafrost could account for a quarter of thawed carbon based on Pliocene–Pleistocene paleoclimate analogue. *Nature Communications*, 13(1), 1–12. <https://doi.org/10.1038/s41467-022-29011-2>

- Csank, A.Z., Tripathi, A.K., Patterson, W.P., Eagle, R.A., Rybczynski, N., Ballantyne, A.P. & Eiler, J.M. (2011) Estimates of Arctic land surface temperatures during the early Pliocene from two novel proxies. *Earth and Planetary Science Letters*, 304(3–4), 291–299. <https://doi.org/10.1016/j.epsl.2011.02.030>
- Daëron, M. (2021) Full propagation of analytical uncertainties in  $\Delta_{47}$  measurements. *Geochemistry, Geophysics, Geosystems*, 22(5), e2020GC009592. <https://doi.org/10.1029/2020GC009592>
- Daëron, M., Blamart, D., Peral, M. & Affek, H.P. (2016) Absolute isotopic abundance ratios and the accuracy of  $\Delta_{47}$  measurements. *Chemical Geology*, 442, 83–96. <https://doi.org/10.1016/j.chemgeo.2016.08.014>
- Das, O., Wang, Y., Donoghue, J., Xu, X., Coor, J., Elsner, J. & Xu, Y. (2013) Reconstruction of paleostorms and paleoenvironment using geochemical proxies archived in the sediments of two coastal lakes in northwest Florida. *Quaternary Science Reviews*, 68, 142–153. <https://doi.org/10.1016/j.quascirev.2013.02.014>
- Davies, A.J. & John, C.M. (2019) The clumped ( $^{13}\text{C}^{18}\text{O}$ ) isotope composition of echinoid calcite: further evidence for “vital effects” in the clumped isotope proxy. *Geochimica et Cosmochimica Acta*, 245, 172–189. <https://doi.org/10.1016/j.gca.2018.07.038>
- Eagle, R.A., Eiler, J.M., Tripathi, A.K., Ries, J.B., Freitas, P.S., Hiebenthal, C., Wanamaker, A.D., Taviani, M., Elliot, M., Marensi, S., Nakamura, K., Ramirez, P. & Roy, K. (2013b) The influence of temperature and seawater carbonate saturation state on  $^{13}\text{C}$ – $^{18}\text{O}$  bond ordering in bivalve mollusks. *Biogeosciences*, 10(7), 4591–4606. <https://doi.org/10.5194/bg-10-4591-2013>
- Eagle, R.A., Risi, C., Mitchell, J.L., Eiler, J.M., Seibt, U., Neelin, J.D., Li, G. & Tripathi, A.K. (2013a) High regional climate sensitivity over continental China constrained by glacial-recent changes in temperature and the hydrological cycle. *Proceedings of the National Academy of Sciences of the United States of America*, 110(22), 8813–8818. <https://doi.org/10.1073/pnas.1213366110>
- Egger, A.E., Ibarra, D.E., Weldon, R., Langridge, R.M., Marion, B., Hall, J., Starratt, S.W. & Rosen, M.R. (2018) Influence of pluvial lake cycles on earthquake recurrence in the northwestern Basin and Range, USA. *Geological Society of America Special Paper*, 536, 1–28. [https://doi.org/10.1130/2018.2536\(07\)](https://doi.org/10.1130/2018.2536(07))
- Epstein, S., Buchsbaum, R., Lowenstam, H.A. & Urey, H.C. (1953) Revised carbonate-water isotopic temperature scale. *Geological Society of America Bulletin*, 64(11), 1315–1326. [https://doi.org/10.1130/0016-7606\(1953\)64\[1315:RCITS\]2.0.CO;2](https://doi.org/10.1130/0016-7606(1953)64[1315:RCITS]2.0.CO;2)
- Esper, J., St. George, S., Anchukaitis, K., D'Arrigo, R., Ljungqvist, F.C., Luterbacher, J., Schneider, L., Stoffel, M., Wilson, R. & Büntgen, U. (2018) Large-scale, millennial-length temperature reconstructions from tree-rings. *Dendrochronologia*, 50, 81–90. <https://doi.org/10.1016/j.dendro.2018.06.001>
- Gallagher, T.M. & Sheldon, N.D. (2013) A new paleothermometer for forest paleosols and its implications for Cenozoic climate. *Geology*, 41(6), 647–650. <https://doi.org/10.1130/G34074.1>
- Ghosh, P., Adkins, J., Affek, H., Balta, B., Guo, W., Schauble, E.A., Schrag, D. & Eiler, J.M. (2006b)  $^{13}\text{C}$ – $^{18}\text{O}$  bonds in carbonate minerals: a new kind of paleothermometer. *Geochimica et Cosmochimica Acta*, 70(6), 1439–1456. <https://doi.org/10.1016/j.gca.2005.11.014>
- Ghosh, P., Garzzone, C.N. & Eiler, J.M. (2006a) Rapid Uplift of the Altiplano Revealed Through  $^{13}\text{C}$ – $^{18}\text{O}$  Bonds in Paleosol Carbonates. *Science*, 311(5760), 511–515. <https://doi.org/10.1126/science.1119365>
- Gierlowski-Kordesch, E.H. (2010) Lacustrine carbonates. *Developments in Sedimentology*, 61, 1–101.
- Grauel, A.-L., Hodell, D.A. & Bernasconi, S.M. (2016) Quantitative estimates of tropical temperature change in lowland Central America during the last 42 ka. *Earth and Planetary Science Letters*, 438, 37–46. <https://doi.org/10.1016/j.epsl.2016.01.001>
- Gwynn, J.W. (2007) Great Salt Lake Brine chemistry databases and reports, 1966–2006. Utah Geological Survey Salt Lake City, UT.
- Hansen, J., Sato, M., Kharechaa, P., Beerling, D., Berner, R., Masson-delmotte, V., Paganid, M., Raymof, M., Royerg, D.L. & Zachosh, J.C. (2008) Target atmospheric  $\text{CO}_2$ : where should humanity aim? *The Open Atmospheric Science Journal*, 2, 217–231. <https://doi.org/10.2174/1874282300802010217>
- Hill, P.S., Schauble, E.A. & Tripathi, A. (2020) Theoretical constraints on the effects of added cations on clumped, oxygen, and carbon isotope signatures of dissolved inorganic carbon species and minerals. *Geochimica et Cosmochimica Acta*, 269, 496–539. <https://doi.org/10.1016/j.gca.2019.10.016>
- Hill, P.S., Tripathi, A.K. & Schauble, E.A. (2014) Theoretical constraints on the effects of pH, salinity, and temperature on clumped isotope signatures of dissolved inorganic carbon species and precipitating carbonate minerals. *Geochimica et Cosmochimica Acta*, 125, 610–652. <https://doi.org/10.1016/j.gca.2013.06.018>
- Horton, T.W., Defliese, W.F., Tripathi, A.K. & Oze, C. (2016) Evaporation induced  $^{18}\text{O}$  and  $^{13}\text{C}$  enrichment in lake systems: a global perspective on hydrologic balance effects. *Quaternary Science Reviews*, 131, 365–379. <https://doi.org/10.1016/j.quascirev.2015.06.030>
- Hren, M.T. & Sheldon, N.D. (2012) Temporal variations in lake water temperature: paleoenvironmental implications of lake carbonate  $\delta^{18}\text{O}$  and temperature records. *Earth and Planetary Science Letters*, 337, 77–84. <https://doi.org/10.1016/j.epsl.2012.05.019>
- Hren, M.T., Sheldon, N.D., Grimes, S.T., Collinson, M.E., Hooker, J.J., Bugler, M. & Lohmann, K.C. (2013) Terrestrial cooling in Northern Europe during the eocene-oligocene transition. *Proceedings of the National Academy of Sciences of the United States of America*, 110(19), 7562–7567. <https://doi.org/10.1073/pnas.1210930110>
- Hudson, A.M., Quade, J., Ali, G., Boyle, D., Bassett, S., Huntington, K.W., De los Santos, M.G., Cohen, A.S., Lin, K. & Wang, X. (2017) Stable C, O and clumped isotope systematics and  $^{14}\text{C}$  geochronology of carbonates from the Quaternary Chewaucan closed-basin lake system, Great Basin, USA: implications for paleoenvironmental reconstructions using carbonates. *Geochimica et Cosmochimica Acta*, 212, 274–302. <https://doi.org/10.1016/j.gca.2017.06.024>
- Huntington, K.W. & Lechler, A.R. (2015) Carbonate clumped isotope thermometry in continental tectonics. *Tectonophysics*, 647–648, 1–20. <https://doi.org/10.1016/j.tecto.2015.02.019>
- Huntington, K.W., Saylor, J., Quade, J. & Hudson, A.M. (2015) High late Miocene–Pliocene elevation of the Zhada Basin, southwestern Tibetan Plateau, from carbonate clumped isotope thermometry. *Geological Society of America Bulletin*, 127(1–2), 181–199. <https://doi.org/10.1130/B31000.1>
- Huntington, K.W., Wernicke, B.P. & Eiler, J.M. (2010) Influence of climate change and uplift on Colorado Plateau paleotemperatures

- from carbonate clumped isotope thermometry: Colorado plateau carbonates. *Tectonics*, 29(3), TC3005. <https://doi.org/10.1029/2009TC002449>
- Ibarra, D.E., Egger, A.E., Weaver, K.L., Harris, C.R. & Maher, K. (2014) Rise and fall of late Pleistocene pluvial lakes in response to reduced evaporation and precipitation: evidence from Lake Surprise, California. *GSA Bulletin*, 126(11–12), 1387–1415. <https://doi.org/10.1130/B31014.1>
- Ingalls, M., Frantz, C.M., Snell, K.E. & Trower, E.J. (2020) Carbonate facies-specific stable isotope data record climate, hydrology, and microbial communities in Great Salt Lake, UT. *Geobiology*, 18(5), 566–593. <https://doi.org/10.1111/gbi.12386>
- Ingalls, M., Rowley, D., Olack, G., Currie, B., Li, S., Schmidt, J., Tremblay, M., Polissar, P., Shuster, D.L., Lin, D. & Colman, A. (2017) Paleocene to Pliocene low-latitude, high-elevation basins of southern Tibet: implications for tectonic models of India-Asia collision, Cenozoic climate, and geochemical weathering. *GSA Bulletin*, 130(1–2), 307–330. <https://doi.org/10.1130/B31723.1>
- John, C.M. & Bowen, D. (2016) Community software for challenging isotope analysis: first applications of “Easotope” to clumped isotopes: community software for challenging isotope analysis. *Rapid Communications in Mass Spectrometry*, 30(21), 2285–2300. <https://doi.org/10.1002/rcm.7720>
- Kato, H., Amekawa, S., Kano, A., Mori, T., Kuwahara, Y. & Quade, J. (2019) Seasonal temperature changes obtained from carbonate clumped isotopes of annually laminated tufas from Japan: discrepancy between natural and synthetic calcites. *Geochimica et Cosmochimica Acta*, 244, 548–564. <https://doi.org/10.1016/j.gca.2018.10.016>
- Kaufman, D., McKay, N., Routson, C., Erb, M., Davis, B., Heiri, O., Jaccard, S., Tierney, J., Dätwyler, C. & Axford, Y. (2020) A global database of Holocene paleotemperature records. *Scientific Data*, 7(1), 1–34. <https://doi.org/10.1038/s41597-020-0445-3>
- Kele, S., Breitenbach, S.F.M., Capezzuoli, E., Meckler, A.N., Ziegler, M., Millan, I.M., Kluge, T., Deák, J., Hanselmann, K., John, C.M., Yan, H., Liu, Z. & Bernasconi, S.M. (2015) Temperature dependence of oxygen- and clumped isotope fractionation in carbonates: a study of travertines and tufas in the 6–95°C temperature range. *Geochimica et Cosmochimica Acta*, 168, 172–192. <https://doi.org/10.1016/j.gca.2015.06.032>
- Kim, S.-T. & O’Neil, J.R. (1997) Equilibrium and nonequilibrium oxygen isotope effects in synthetic carbonates. *Geochimica et Cosmochimica Acta*, 61(16), 3461–3475. [https://doi.org/10.1016/S0016-7037\(97\)00169-5](https://doi.org/10.1016/S0016-7037(97)00169-5)
- Kim, S.-T., O’Neil, J.R., Hillaire-Marcel, C. & Mucci, A. (2007) Oxygen isotope fractionation between synthetic aragonite and water: influence of temperature and Mg<sup>2+</sup> concentration. *Geochimica et Cosmochimica Acta*, 71(19), 4704–4715. <https://doi.org/10.1016/j.gca.2007.04.019>
- Kimball, J., Eagle, R. & Dunbar, R. (2016) Carbonate “clumped” isotope signatures in aragonitic scleractinian and calcitic gorgonian deep-sea corals. *Biogeosciences*, 13(23), 6487–6505. <https://doi.org/10.5194/bg-13-6487-2016>
- Li, H., Liu, X., Arnold, A., Elliott, B., Flores, R., Kelley, A.M. & Tripathi, A. (2021) Mass 47 clumped isotope signatures in modern lacustrine authigenic carbonates in Western China and other regions and implications for paleotemperature and paleoelevation reconstructions. *Earth and Planetary Science Letters*, 562, 116840. <https://doi.org/10.1016/j.epsl.2021.116840>
- Li, H., Liu, X., Tripathi, A., Feng, S., Elliott, B., Whicker, C., Arnold, A. & Kelley, A.M. (2020) Factors controlling the oxygen isotopic composition of lacustrine authigenic carbonates in Western China: implications for paleoclimate reconstructions. *Scientific Reports*, 10(1), 16370. <https://doi.org/10.1038/s41598-020-73422-4>
- Li, L., Fan, M., Davila, N., Jesmok, G., Mitsunaga, B., Tripathi, A. & Orme, D. (2019) Carbonate stable and clumped isotopic evidence for late Eocene moderate to high elevation of the east-central Tibetan Plateau and its geodynamic implications. *GSA Bulletin*, 131(5–6), 831–844. <https://doi.org/10.1130/B32060.1>
- Li, X., Zhou, X., Liu, W., Wang, Z., He, Y. & Xu, L. (2016) Carbon and oxygen isotopic records from Lake Tuosu over the last 120 years in the Qaidam Basin, Northwestern China: the implications for paleoenvironmental reconstruction. *Global and Planetary Change*, 141, 54–62. <https://doi.org/10.1016/j.gloplacha.2016.04.006>
- Lucarelli, J.K., Carroll, H.M., Ulrich, R.N., Elliott, B.M., Coplen, T.B., Eagle, R.A. & Tripathi, A. (2023) Equilibrated gas and carbonate standard-derived dual ( $\Delta_{47}$  and  $\Delta_{48}$ ) clumped isotope values. *Geochemistry, Geophysics, Geosystems*, 24(2), e2022GC010458. <https://doi.org/10.1029/2022GC010458>
- Mackey, T.J., Sumner, D.Y., Hawes, I., Leidman, S.Z., Andersen, D.T. & Jungblut, A.D. (2018) Stromatolite records of environmental change in perennially ice-covered Lake Joyce, McMurdo Dry Valleys, Antarctica. *Biogeochemistry*, 137(1), 73–92. <https://doi.org/10.1007/s10533-017-0402-1>
- Meckler, A.N., Vonhof, H. & Martínez-García, A. (2021) Temperature reconstructions using speleothems. *Elements*, 17(2), 101–106. <https://doi.org/10.2138/gselements.17.2.101>
- Pace, A., Bourillot, R., Bouton, A., Vennin, E., Galaup, S., Bundeleva, I., Patrier, P., Dupraz, C., Thomazo, C., Sansjofre, P., Yokoyama, Y., Franceschi, M., Anguy, Y., Pigot, L., Virgone, A. & Visscher, P.T. (2016) Microbial and diagenetic steps leading to the mineralisation of Great Salt Lake microbialites. *Scientific Reports*, 6(1), 31495. <https://doi.org/10.1038/srep31495>
- Paradis, O.P. (2019) Great Salt Lake ooids: insights into rate of formation, potential as paleoenvironmental archives, and biogenicity. PhD Thesis, University of Southern California.
- Passey, B.H., Levin, N.E., Cerling, T.E., Brown, F.H. & Eiler, J.M. (2010) High-temperature environments of human evolution in East Africa based on bond ordering in paleosol carbonates. *Proceedings of the National Academy of Sciences of the United States of America*, 107(25), 11245–11249. <https://doi.org/10.1073/pnas.1001824107>
- Petersen, S.V., Defliese, W.F., Saenger, C., Daëron, M., Huntington, K.W., John, C.M., Kelson, J.R., Bernasconi, S.M., Colman, A.S., Kluge, T., Olack, G.A., Schauer, A.J., Bajnai, D., Bonifacie, M., Breitenbach, S.F.M., Fiebig, J., Fernandez, A.B., Henkes, G.A., Hodell, D., Katz, A., Kele, S., Lohmann, K.C., Passey, B.H., Peral, M.Y., Petrizzo, D.A., Rosenheim, B.E., Tripathi, A., Venturelli, R., Young, E.D. & Winkelstern, I.Z. (2019) Effects of improved <sup>17</sup>O correction on interlaboratory agreement in clumped isotope calibrations, estimates of mineral-specific offsets, and temperature dependence of acid digestion fractionation. *Geochemistry, Geophysics, Geosystems*, 20(7), 3495–3519. <https://doi.org/10.1029/2018GC008127>
- Petryshyn, V.A., Lim, D., Laval, B.L., Brady, A., Slater, G. & Tripathi, A.K. (2015) Reconstruction of limnology and microbialite formation conditions from carbonate clumped isotope



- thermometry. *Geobiology*, 13(1), 53–67. <https://doi.org/10.1111/gbi.12121>
- Platt, N.H. & Wright, V.P. (2009) Lacustrine carbonates: facies models, facies distributions and hydrocarbon aspects. In: Anadón, P., Cabrera, L.L. & Kelts, K. (Eds.) *Lacustrine Facies Analysis. Special Publication of the International Association of Sedimentologists*. Ghent, Belgium: International Association of Sedimentologists, John Wiley & Sons, Ltd, pp. 57–74. <https://doi.org/10.1002/9781444303919.ch3>
- Poage, M.A. & Chamberlain, C.P. (2001) Empirical relationships between elevation and the stable isotope composition of precipitation and surface waters: considerations for studies of paleoelevation change. *American Journal of Science*, 301(1), 1–15. <https://doi.org/10.2475/ajs.301.1.1>
- Powers, L., Werne, J.P., Vanderwoude, A.J., Sinninghe Damsté, J.S., Hopmans, E.C. & Schouten, S. (2010) Applicability and calibration of the TEX86 paleothermometer in lakes. *Organic Geochemistry*, 41(4), 404–413. <https://doi.org/10.1016/j.orggeochem.2009.11.009>
- Quade, J., Eiler, J., Daëron, M. & Achyuthan, H. (2013) The clumped isotope geothermometer in soil and paleosol carbonate. *Geochimica et Cosmochimica Acta*, 105, 92–107. <https://doi.org/10.1016/j.gca.2012.11.031>
- R Core Team. (2022) *R: a language and environment for statistical computing*. Vienna, Austria: R Foundation for Statistical Computing. <https://www.R-project.org/>
- Richter, F., Garzzone, C.N., Liu, W., Qiang, X., Chang, H., Cheng, F., Li, X. & Tripathi, A. (2022) Plio-Pleistocene cooling of the northeastern Tibetan Plateau due to global climate change and surface uplift. *GSA Bulletin*, 135(5–6), 1327–1343. <https://doi.org/10.1130/B36302.1>
- Román Palacios, C., Carroll, H., Arnold, A., Flores, R., Petersen, S., McKinnon, K. & Tripathi, A. (2021) BayClump: Bayesian calibration and temperature reconstructions for clumped isotope thermometry. <https://doi.org/10.1002/essoar.10507995.1>
- Rowley, D.B. & Garzzone, C.N. (2007) Stable Isotope-Based Paleothermometry. *Annual Review of Earth and Planetary Sciences*, 35(1), 463–508. <https://doi.org/10.1146/annurev.earth.35.031306.140155>
- Saenger, C., Affek, H.P., Felis, T., Thiagarajan, N., Lough, J.M. & Holcomb, M. (2012) Carbonate clumped isotope variability in shallow water corals: temperature dependence and growth-related vital effects. *Geochimica et Cosmochimica Acta*, 99, 224–242. <https://doi.org/10.1016/j.gca.2012.09.035>
- Santi, L., Arnold, A., Mering, J., Arnold, D., Tripathi, A., Whicker, C. & Oviatt, C.G. (2019) Lake level fluctuations in the Northern Great Basin for the last 25,000 years. In: *Exploring ends of eras in the Eastern Mojave Desert: 2019 Desert Symposium field guide and proceedings*. Running Springs, California: Desert Symposium Inc, pp. 176–186. <https://doi.org/10.31223/osf.io/6as7t>
- Santi, L., Arnold, A.J., Ibarra, D.E., Whicker, C.A., Mering, J.A., Lomarda, R.B., Lora, J.M. & Tripathi, A. (2020) Clumped isotope constraints on changes in latest Pleistocene hydroclimate in the northwestern Great Basin: Lake Surprise, California. *GSA Bulletin*, 132(11–12), 2669–2683. <https://doi.org/10.1130/B35484.1>
- Schauble, E.A., Ghosh, P. & Eiler, J.M. (2006) Preferential formation of  $^{13}\text{C}$ – $^{18}\text{O}$  bonds in carbonate minerals, estimated using first-principles lattice dynamics. *Geochimica et Cosmochimica Acta*, 70(10), 2510–2529. <https://doi.org/10.1016/j.gca.2006.02.011>
- Schelske, C.L. & Hodell, D.A. (1995) Using carbon isotopes of bulk sedimentary organic matter to reconstruct the history of nutrient loading and eutrophication in Lake Erie. *Limnology and Oceanography*, 40(5), 918–929. <https://doi.org/10.4319/lo.1995.40.5.0918>
- Spencer, C. & Kim, S.-T. (2015) Carbonate clumped isotope paleothermometry: a review of recent advances in  $\text{CO}_2$  gas evolution, purification, measurement and standardization techniques. *Geosciences Journal*, 19(2), 357–374. <https://doi.org/10.1007/s12303-015-0018-1>
- Spooner, P.T., Guo, W., Robinson, L.F., Thiagarajan, N., Hendry, K.R., Rosenheim, B.E. & Leng, M.J. (2016) Clumped isotope composition of cold-water corals: a role for vital effects? *Geochimica et Cosmochimica Acta*, 179, 123–141. <https://doi.org/10.1016/j.gca.2016.01.023>
- Stuiver, M. & Grootes, P.M. (2000) GISP2 oxygen isotope ratios. *Quaternary Research*, 53(3), 277–284. <https://doi.org/10.1006/qres.2000.2127>
- Stute, M. & Schlosser, P. (2000) Atmospheric Noble Gases. In: Cook, P.G. & Herczeg, A.L. (Eds.) *Environmental Tracers in Subsurface Hydrology*. Boston, MA: Springer US, pp. 349–377. [https://doi.org/10.1007/978-1-4615-4557-6\\_11](https://doi.org/10.1007/978-1-4615-4557-6_11)
- Swart, P.K., Burns, S.J. & Leder, J.J. (1991) Fractionation of the stable isotopes of oxygen and carbon in carbon dioxide during the reaction of calcite with phosphoric acid as a function of temperature and technique. *Chemical Geology: Isotope Geoscience Section*, 86(2), 89–96. [https://doi.org/10.1016/0168-9622\(91\)90055-2](https://doi.org/10.1016/0168-9622(91)90055-2)
- Tang, J., Dietzel, M., Fernandez, A., Tripathi, A.K. & Rosenheim, B.E. (2014) Evaluation of kinetic effects on clumped isotope fractionation ( $\Delta_{47}$ ) during inorganic calcite precipitation. *Geochimica et Cosmochimica Acta*, 134, 120–136. <https://doi.org/10.1016/j.gca.2014.03.005>
- Tripathi, A.K., Eagle, R.A., Thiagarajan, N., Gagnon, A.C., Bauch, H., Halloran, P.R. & Eiler, J.M. (2010)  $^{13}\text{C}$ – $^{18}\text{O}$  isotope signatures and “clumped isotope” thermometry in foraminifera and coccoliths. *Geochimica et Cosmochimica Acta*, 74(20), 5697–5717. <https://doi.org/10.1016/j.gca.2010.07.006>
- Tripathi, A.K., Hill, P.S., Eagle, R.A., Mosenfelder, J.L., Tang, J., Schauble, E.A., Eiler, J.M., Zeebe, R.E., Uchikawa, J., Coplen, T.B., Ries, J.B. & Henry, D. (2015) Beyond temperature: clumped isotope signatures in dissolved inorganic carbon species and the influence of solution chemistry on carbonate mineral composition. *Geochimica et Cosmochimica Acta*, 166, 344–371. <https://doi.org/10.1016/j.gca.2015.06.021>
- Tripathi, A.K., Sahany, S., Pittman, D., Eagle, R.A., Neelin, J.D., Mitchell, J.L. & Beaufort, L. (2014) Modern and glacial tropical snowlines controlled by sea surface temperature and atmospheric mixing. *Nature Geoscience*, 7(3), 205–209. <https://doi.org/10.1038/ngeo2082>
- Upadhyay, D., Lucarelli, J., Arnold, A., Flores, R., Bricker, H., Ulrich, R.N., Jesmok, G., Santi, L., Defliese, W., Eagle, R.A., Carroll, H.M., Bateman, J.B., Petryshyn, V., Loyd, S.J., Tang, J., Priyadarshi, A., Elliott, B. & Tripathi, A. (2021) Carbonate clumped isotope analysis ( $\Delta_{47}$ ) of 21 carbonate standards determined via gas-source isotope-ratio mass spectrometry on four instrumental configurations using carbonate-based standardization and multiyear data sets. *Rapid Communications in Mass Spectrometry*, 35(17), e9143. <https://doi.org/10.1002/rcm.9143>

- Urey, H.C. (1947) The thermodynamic properties of isotopic substances. *Journal of the Chemical Society*, 562–581. <https://doi.org/10.1039/JR9470000562>
- Vasconcelos, C., McKenzie, J.A., Warthmann, R. & Bernasconi, S.M. (2005) Calibration of the  $\delta^{18}\text{O}$  paleothermometer for dolomite precipitated in microbial cultures and natural environments. *Geology*, 33(4), 317–320. <https://doi.org/10.1130/G20992.1>
- Versteegh, E.A., Vonhof, H.B., Troelstra, S.R., Kaandorp, R.J. & Kroon, D. (2010) Seasonally resolved growth of freshwater bivalves determined by oxygen and carbon isotope shell chemistry. *Geochemistry, Geophysics, Geosystems*, 11(8), Q08022. <https://doi.org/10.1029/2009GC002961>
- Wang, Y., Passey, B., Roy, R., Deng, T., Jiang, S., Hannold, C., Wang, X., Lochner, E. & Tripathi, A. (2021) Clumped isotope thermometry of modern and fossil snail shells from the Himalayan-Tibetan Plateau: implications for paleoclimate and paleoelevation reconstructions. *GSA Bulletin*, 133(7–8), 1370–1380. <https://doi.org/10.1130/B35784.1>
- Wilf, P. (1997) When are leaves good thermometers? A new case for Leaf Margin Analysis. *Paleobiology*, 23(3), 373–390. <https://doi.org/10.1017/S0094837300019746>
- Wroczynna, C., Meyer, J., Dietzel, M. & Piller, W.E. (2022) Neotropical ostracode oxygen and carbon isotope signatures: implications for calcification conditions. *Biogeochemistry*, 159(1), 103–138. <https://doi.org/10.1007/s10533-022-00917-9>
- Xu, H., Ai, L., Tan, L. & An, Z. (2006) Stable isotopes in bulk carbonates and organic matter in recent sediments of Lake Qinghai and their climatic implications. *Chemical Geology*, 235(3), 262–275. <https://doi.org/10.1016/j.chemgeo.2006.07.005>
- Zaarur, S., Affek, H.P. & Stein, M. (2016) Last glacial-Holocene temperatures and hydrology of the Sea of Galilee and Hula Valley from clumped isotopes in *Melanopsis* shells. *Geochimica et Cosmochimica Acta*, 179, 142–155. <https://doi.org/10.1016/j.gca.2015.12.034>

## SUPPORTING INFORMATION

Additional supporting information can be found online in the Supporting Information section at the end of this article.

**How to cite this article:** Arnold, A., Mering, J., Santi, L., Román-Palacios, C., Li, H., Petryshyn, V. et al. (2024) Comparative clumped isotope temperature relationships in freshwater carbonates. *The Depositional Record*, 00, 1–26. Available from: <https://doi.org/10.1002/dep2.312>